Geochemical Perspectives Letters

Copper isotope evidence for large-scale sulphide fractionation during Earth's differentiation

P.S. Savage[1, 2, 3*], F. Moynier[1], H. Chen[4], G. Shofner[1], J. Siebert[1], J. Badro[1, 5], I.S. Puchtel[6]

OPEN ACCESS

doi: 10.7185/geochemlet.1506

Abstract

The differentiation of Earth into a metallic core and silicate mantle left its signature on the chemical and isotopic composition of the bulk silicate Earth (BSE). This is seen in the depletion of siderophile (metal-loving) relative to lithophile (rock-loving) elements in Earth's mantle as well as the silicon isotope offset between primitive meteorites (*i.e.* bulk Earth) and BSE, which is generally interpreted as a proof that Si is present in Earth's core. Another putative light element in Earth's core is sulphur; however, estimates of core S abundance vary significantly and, due to its volatile nature, no unequivocal S isotopic signature for core fractionation has thus far been detected. Here we present new high precision isotopic data for Cu, a chalcophile (sulphur-loving) element, which shows that Earth's mantle is isotopically fractionated relative to bulk Earth. Results from high pressure equilibration experiments suggest that the sense of Cu isotopic fractionation between BSE and bulk Earth requires that a sulphide-rich liquid segregated from Earth's mantle during differentiation, which likely entered the core. Such an early-stage removal of a sulphide-rich phase from the mantle presents a possible solution to the long-standing 1st terrestrial lead paradox.

Received 18 March 2015 | Accepted 10 April 2015 | Published 4 June 2015

1. Institut de Physique du Globe de Paris, Institut Universitaire de France, Sorbonne Paris Cité – Université Paris Diderot, UMR CNRS 7154, 1 rue Jussieu, 75005 Paris, France
2. Department of Earth Sciences, Durham University, Science Labs, Durham DH1 3LE, UK
3. Department of Earth and Environmental Sciences, University of St. Andrews, Irvine Building, St. Andrews, KY16 9AL, UK
* Corresponding author: p.s.savage@dur.ac.uk
4. Department of Earth and Planetary Sciences and McDonnell Center for the Space Sciences, Washington University in St. Louis, One Brookings Drive, St. Louis, MO 63130, USA
5. Earth and Planetary Science Laboratory, Ecole Polytechnique Federale de Lausanne, CH-1015 Lausanne, Switzerland
6. Department of Geology, University of Maryland, College Park, Maryland 20742, USA

Letter

The budget of light elements in Earth's core is a long-standing geochemical problem (Poirier, 1994), as constraining such elements and their abundances can tell us much about the physiochemical conditions of Earth's differentiation. Sulphur is often cited as one such element: cosmochemical estimates suggest that the core contains ~2 wt. % S (Dreibus and Palme, 1996); sulphur in the core is seemingly necessary to explain mantle W and Mo abundances (Wade *et al.*, 2012) and can explain the disparity between the radiometric Pb and W isotope ages of the mantle (Wood and Halliday, 2005). However, recent molecular dynamics estimates suggest S may not be present at all in the core (Badro *et al.*, 2014); also, it is unclear as to whether S entered the core as an iron alloy, or as a discrete sulphide phase (O'Neill, 1991). Further complications stem from the fact that late addition of extra-terrestrial S to the mantle, post-core formation, should overwhelm any pre-existing S (isotope) signature (the "late veneer"; Holzheid *et al.*, 2000; Wang *et al.*, 2013). In an effort to investigate the role of S during Earth's differentiation, we have investigated the Cu isotope compositions of bulk Earth and BSE; this is because Cu is siderophile and strongly chalcophile (~2/3 of Earth's Cu is thought to be in the core; Palme and O'Neill, 2014, McDonough, 2003) but is less volatile than S, so is abundant enough in Earth's mantle to have been largely unaffected by a late veneer.

To begin with, it was necessary to obtain robust Cu isotope compositions for both BSE and bulk Earth. To this end, we measured the Cu isotope composition of 88 extra-terrestrial and terrestrial samples using high precision multi-collector inductively coupled plasma mass spectrometry (MC-ICPMS; see Supplementary Information for methods and data tables) and combined these results with pre-existing literature data.

Choosing samples to constrain the Cu isotope composition of BSE is not trivial, due to the specific behaviour of Cu during mantle melting. The concentration of Cu in a mantle melt is predominantly controlled by the consumption of sulphide phases by such a melt (Lee *et al.*, 2012). If melt fraction remains below ~25 %, residual sulphides should retain Cu, which could potentially give rise to isotopic fractionation. With this in mind, two lithologies were initially chosen to constrain the copper isotopic composition of BSE. The first were komatiites, mantle-derived ultramafic lavas generated by high degrees (>25 %) of mantle melting and typically found in Archaean terrains (Arndt, 2008). In this study, we analysed komatiite samples from two localities; 2.4 Ga Vetreny Belt (Baltic Shield) and 2.7 Ga Belingwe (South Africa). The second were "fertile" orogenic lherzolites from Lanzo (Italy) and Horoman (Japan); that is, samples of the mantle that appear to have undergone little to no melt depletion. These data were augmented by Cu isotope analyses of mid-ocean ridge basalts (MORB), which are typically formed by fairly high (10-15 %) degrees of melting of upper mantle. We also include data from a variety of ocean island basalt samples to investigate the possibility of Cu isotope mantle heterogeneities (see Supplementary Information for all sample information).

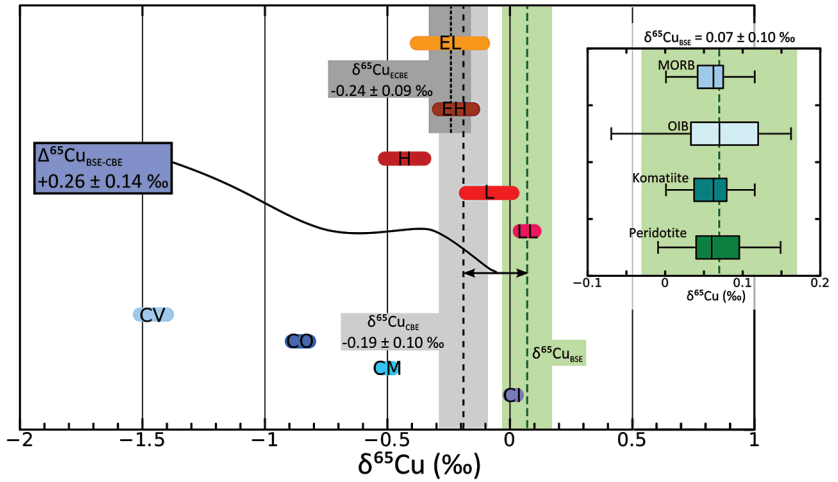

Figure 1 Copper isotope range of the primitive (chondritic) meteorite groups. Inset: Box and whisker plot showing the range of Cu isotope compositions for the terrestrial samples used in constraining the BSE Cu isotope composition. Green box and dotted line represents the composition of BSE, light grey box and long dashes represent the composition of "chondritic bulk Earth" (CBE), dark grey box and short dashes represent the composition of "enstatite chondrite bulk Earth" (ECBE). Errors on the estimates are all 2 s.d.

The Cu isotope compositions of terrestrial basalts and ultramafic rocks define a limited range (–0.07 ‰ < δ^{65}Cu < +0.16 ‰; Fig. 1, $\delta^{65}Cu = [(^{65}Cu/^{63}Cu_{sample} / ^{65}Cu/^{63}Cu_{std.}) - 1] \times 1000$; where std. is NIST SRM976). Despite the potential for Cu isotope fractionation through sulphide retention, each sample group is statistically identical and the data are normally distributed (Supplementary Information), providing a robust and precise average BSE Cu isotope composition of $\delta^{65}Cu_{BSE}$ = 0.07 ± 0.10 ‰ (2 s.d.).

It is of course impossible to obtain a sample of the 'bulk Earth' and hence, like many studies before ours, we assume that bulk Earth formed from primitive (chondritic) meteorites (*e.g.*, Palme and O'Neill, 2014). The issue then is to decide which group(s) of meteorites best represents Earth, in terms of its Cu budget. This is particularly important, as the range of chondrite Cu isotope compositions span a wide range (–1.45 ‰ < δ^{65}Cu < +0.07 ‰, Fig. 1; Luck *et al.*, 2005), thus we now discuss a number of model-dependent scenarios.

a) The Earth's Cu budget was established early in Earth's accretion: Like Cu, large isotope variations also exist in systems such as O, Ti, Cr, Ru, Ca etc., suggesting that no single chondrite group represents a perfect match to Earth, and many workers posit a mixture. Based on modelling of Fitoussi and Bourdon (2012), we calculate a chondritic bulk Earth (CBE) value of $\delta^{65}Cu_{CBE}$ = –0.19 ± 0.10 ‰ (2 s.d., Fig. 1). Another approach is to utilise the enstatite chondrites; despite being chemically dissimilar, these meteorites are identical to the Earth for most isotope systems (Dauphas *et al.*, 2014) and many models suggest that the material that accreted to form the Earth contained a large proportion of enstatite chondrite-like planetesimals (Dauphas *et al.*, 2014). Both enstatite chondrites groups have similar ranges as well as having identical δ^{65}Cu values (Fig. 1); a mixture of EH and EL chondrites gives an enstatite chondrite bulk Earth (ECBE) of δ^{65}Cu = –0.24 ± 0.09 ‰ (2 s.d., Fig. 1), identical to $\delta^{65}Cu_{CBE}$.

b) The Earth's Cu was delivered late, as a result of the Moon-forming giant impact: The mantle budget of Cu and other moderately volatile elements may be dominated by the final 10 % of material accreted to Earth, associated for example with the Moon-forming giant impactor, Theia (Albarède, 2009). The Cu in the mantle, therefore, would have escaped the effects of all but the final stages of planetary differentiation, as Hf-W isotope data suggests that the majority of the core had formed by the time of impact (Kleine *et al.*, 2010). Work on Ag isotopes by Schönbächler *et al.* (2010) seemed to indicate that the impactor material was dominated by CI-like material. If this is the case, then our data would seem to support their model; our estimate for BSE is almost identical to the Cu isotope composition of CI chondrites. However, more recent isotope data seems to rule out a CI-like impactor; in particular, precise lunar O isotope data suggests that the impactor had an enstatite chondrite isotope signature (Herwartz *et al.*, 2014). In this instance, again, the enstatite chondrite model would seem most representative of bulk Earth.

Accepting either model 'a' or 'b' above, the bulk Earth Cu isotope composition lies somewhere between δ^{65}Cu = –0.19 ± 0.10 ‰ and –0.24 ± 0.09 ‰. Therefore, in terms of Cu isotopes, BSE is enriched in the heavy Cu isotope compared to bulk Earth, with a minimum offset (taking bulk Earth to be –0.19 ‰) of +0.26 ± 0.14 ‰ (2 s.d., Fig. 1). This suggests that some process related to planetary differentiation and accretion has affected the Cu isotope composition of Earth's mantle; we now consider the two most likely culprits: volatile loss of Cu, and core formation.

Preferential removal of the lighter Cu isotope during volatile loss could lead to enrichment in isotopically heavy Cu in Earth's mantle. This, however, can be discounted by considering the Zn isotope system. Zinc is more volatile and less siderophile/chalcophile than Cu (Lodders, 2003); like all moderately volatile, lithophile elements, Earth's mantle is depleted in Zn compared to most chondrite groups suggesting partial loss or incomplete accretion (Palme and O'Neill, 2014). However, the bulk Earth Zn isotope composition is equal to or lighter than those same meteorites (Albarède, 2009; Chen *et al.*, 2013), *i.e.* contrary to the isotope effect predicted by volatile loss. Hence whichever process(es) resulted in the volatility-related depletion of Zn in Earth's mantle did not affect its isotopes. It is therefore unlikely that such a process can explain the heavy Cu isotope enrichment in BSE.

Planetary differentiation is therefore the most likely explanation for the Cu isotope difference between BSE and bulk Earth. To further investigate the behaviour of Cu isotopes during core formation, *i.e.* metal-silicate and sulphide-silicate equilibration, we performed a preliminary series of high-pressure, high temperature experiments wherein natural basalt rock powder, doped with Cu (as either metal or oxide) was equilibrated with either pure Fe metal or stoichiometric FeS under fully molten conditions (see Supplementary Information). In the metal-silicate experiments, the direction of isotopic fractionation between the two phases ($\Delta^{65}Cu_{metal\text{-}silicate}$) was always slightly positive, varying little with temperature (~ +0.1 ‰). Crucially, in the sulphide-silicate experiments the sense of fractionation is negative, opposite and with a larger magnitude to that of metal-silicate equilibration (> −0.5 ‰). These data agree with the sense of Cu isotope fractionation between metal, silicate and sulphide measured in iron meteorites (Williams and Archer, 2011), as well as the extremely light Cu isotope compositions measured in secondary sulphide minerals (Markl *et al.*, 2006). Therefore, the positive Cu isotope difference between BSE and bulk Earth cannot be due to metal-silicate fractionation, because the isotopic fractionation has the incorrect sense. Instead, Earth's "missing" light Cu must be stored in a sulphide-rich reservoir.

Mantle sulphides are a potential explanation; however, given the relative Cu isotope homogeneity of mantle-derived lithologies (Fig. 1) as well as the fact that a typical peridotite contains >90 % of its Cu in sulphides (Lee *et al.*, 2012), this requires that a relatively significant budget of Cu is stored in sulphides that are never sampled by mantle melting or by tectonic exhumation. This does not seem to be the case: for instance, komatiites, which formed via high degrees of partial melting (such that at least 95 % of the Cu in the mantle source should be transferred to the melt), have Cu isotope compositions equal to that of orogenic lherzolites, which are (arguably) direct samples of the mantle. Komatiites also provide a temporal view on mantle composition and suggest that the Cu isotope composition of BSE was established at least as far back as 2.7 Ga, the age of our oldest sample. Similarly, ocean island basalts, which potentially sample sulphide-rich pyroxenites, show no evidence for significant Cu isotope mantle heterogeneity (Fig. 1). The lower continental crust is also a possible reservoir for isotopically light Cu sulphides – however, even if the bulk Cu concentration in the lower continental crust was three times current estimates, it would only represent ~0.6 wt. % of BSE Cu and so would require an unfeasibly light composition ($\delta^{65}Cu$ < −40 ‰). Hence, sulphides in the mantle or crust may host some isotopically light Cu, but are apparently not abundant enough to account for the significant Cu isotope offset between BSE and bulk Earth.

An alternative explanation is the early-stage formation of a sulphide-rich (Fe-O-S) liquid in the mantle, as the final volatile-rich residue after crystallisation of a magma ocean; this is often called the "Hadean Matte" (HM; Fig. 2; O'Neill, 1991). Given its higher density compared to ambient mantle, a HM should pond at the core/mantle boundary and, potentially, admix into the core, isolating it from subsequent re-equilibration. Such a reservoir has been invoked to explain

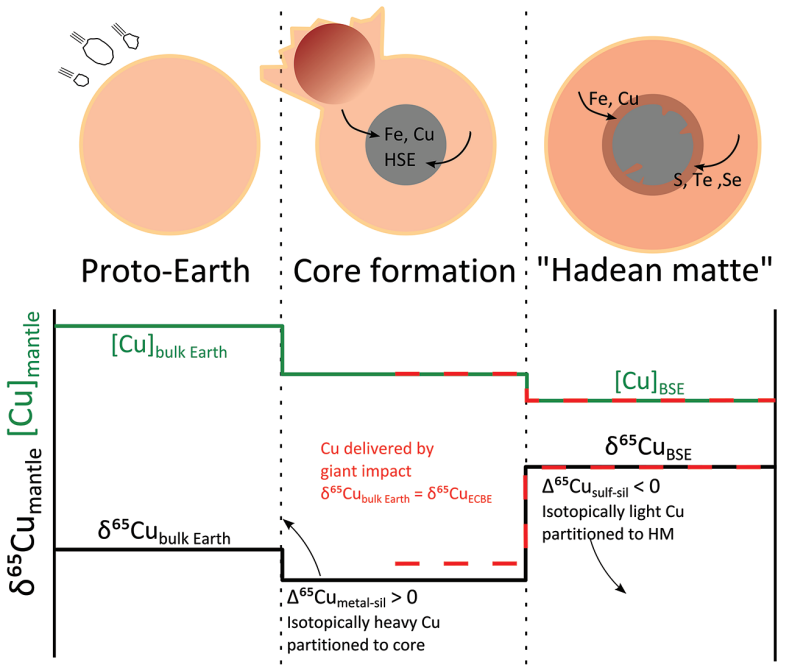

Figure 2 Schematic evolution of Cu concentration and isotopic composition of Earth's mantle as modelled in this contribution. Earth accretes as a mixture of chondrites such that the bulk Earth Cu isotope composition is $\delta^{65}Cu_{CBE}$. Core formation sequesters ~60 % of Earth's Cu in the metal phase, which is enriched in the heavy isotope, driving Earth's mantle to a lighter composition. The formation of a Fe-O-S layer, the "Hadean Matte", sequesters isotopically light Cu, driving Earth's mantle to its present day composition ($\delta^{65}Cu_{BSE}$). Alternatively, Cu is delivered by an enstatite chondrite-like Giant Impactor, and mantle Cu only experiences sulphide-silicate equilibration.

moderately siderophile element abundances in the mantle (O'Neill, 1991) and the mismatch of various core formation chronometers (Wood and Halliday, 2005), and could host significant amounts of Cu. To this end, we have attempted to calculate the mass and composition of a Hadean Matte needed to balance the Cu isotope offset between BSE and bulk Earth. Following previous models, the HM should form after segregation of the majority (99 %) of the core; as such we have used a simple two-stage model, starting from a chondritic ($\delta^{65}Cu_{CBE}$) proto-Earth, where Cu is first partitioned into the core (metal-silicate equilibration), then a sulphide phase (Fig. 2). This is based on model 'a' above, *i.e.* Earth's Cu budget was established early in Earth's accretion. Assuming instead that Earth's mantle Cu was delivered by an enstatite chondrite-like Giant impactor (model 'b' above) does not significantly change the modelling, except that mantle Cu does not experience major metal-silicate equilibration, only sulphide-silicate equilibration (Fig. 2).

A condition of the model 'a' is that the Cu normally assumed to be in Earth's core is now apportioned between HM and core. Fixing a range of likely Cu concentrations in the HM, we calculated the remaining core [Cu] as a function of HM mass (or thickness, assuming a fixed density). This relationship is shown in Figure 3a, wherein the amount of Cu in the core reduces as the HM thickness and Cu concentration increases. The value of $[Cu]_{core}$ should not fall below 120 ppm because Cu is also siderophile (Siebert *et al.*, 2013), which predicts a maximum HM thickness of ~35 km.

We then calculated the Cu isotope composition for each HM scenario required to drive the equilibrating silicate (*i.e.* the mantle) towards the modern-day BSE value. This is shown in Figure 3b, where a smaller HM results in a more negative HM Cu isotope composition. We calculate a range of HM Cu isotope compositions because our preliminary experiments were simply used to assess the sense, not the magnitude of isotope fractionation; however, because large isotope fractionations (> 2 ‰) are not expected at the temperatures associated with the formation of a HM (3000-4000 K), a minimum thickness of ~2 km is predicted, even for the most Cu-rich HM. The maximum size for each HM as controlled by its Cu concentration corresponds to a minimum $\Delta^{65}Cu_{sulphide\text{-}silicate}$ value of ~ –0.6 ‰. To further constrain this model, further work is required to accurately parameterise Cu isotope fractionation factors, but these model predictions are in general agreement with our experimental data (Supplementary Information).

Admixing a Fe-O-S liquid into Earth's core will affect core composition, specifically with regard to the light elements S and O. Given the constraints provided above (HM mass ≤ 1.6 % of Earth's core), addition of a HM to the core will have a small effect on the core O composition (< 0.25 wt. % addition); for S, the effect is more significant – our model suggests that up to ~0.5 wt. % S could be added (Fig. 3a), which is in line with recent estimates based on molecular dynamics (Badro *et al.*, 2014) and siderophile element partitioning studies (Siebert *et al.*, 2013) – of course, this does not preclude further core addition of S as a metal alloy.

Finally, we estimate the effect that removal of the HM could have on mantle lead isotope composition. Lead can be strongly chalcophile, and an early fractionation of isotopically primitive Pb by a sulphide-rich phase is often cited as a solution to the 1st terrestrial Pb paradox; that is, the observation that, in $^{206}Pb/^{204}Pb$ vs. $^{207}Pb/^{204}Pb$ space, most mantle-derived rocks, continental sediments etc. plot to the right of the terrestrial geochron (either the meteoritic, 4.568 Ga geochron or the later Hf-W core formation cessation age of ~4.53 Ga, Fig. 4; Kramers and Tolstikhin, 1997). Modelling the evolution of mantle Pb isotope composition resulting from two fractionation events, metal-silicate equilibration at 50 Ma and sulphide-silicate equilibration at 100 Ma (following Galer and Goldstein, 1996; see Supplementary Information for details), predicts a present-day mantle Pb isotopic composition that is comparable to empirical estimates for BSE, albeit the more unradiogenic ones (Fig. 4; Halliday, 2004) as well as the Pb composition of the ancient primitive mantle as estimated using flood basalts (Jackson and Carlson, 2011). Therefore, this does not preclude further unradiogenic Pb reservoirs, such as sulphides in refractory mantle phases (Burton *et al.*, 2012) or late accretion of mantle Pb (Albarède, 2009).

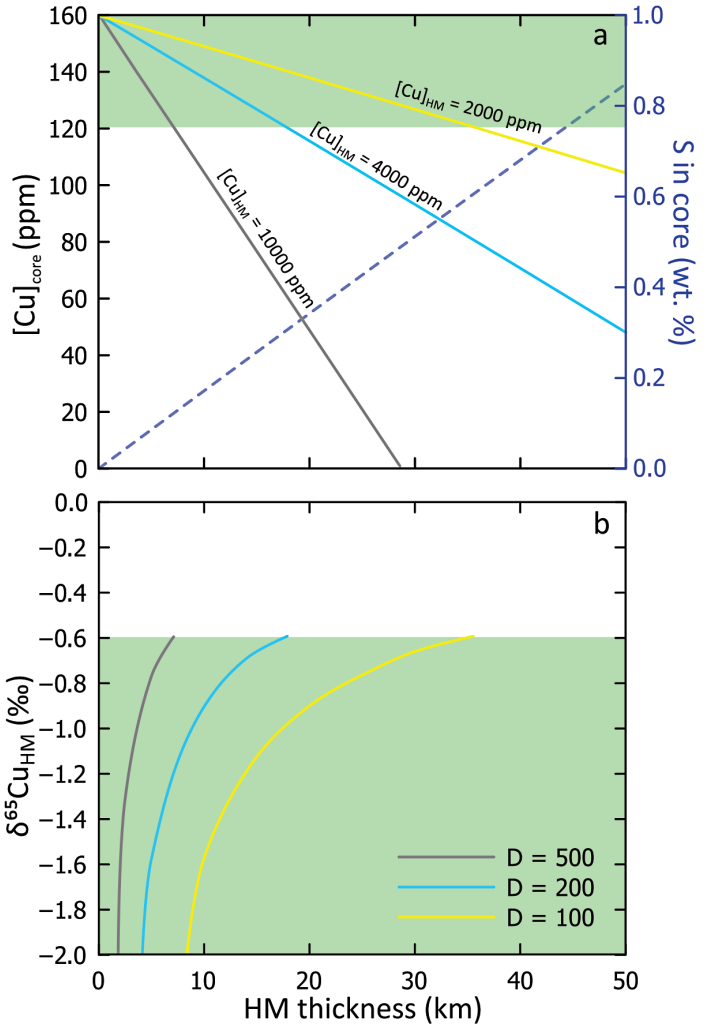

Figure 3 Results of modelled effects of removal of a "Hadean Matte" from the mantle. The effects on a) Cu concentration of Earth's core and b) required Cu isotope composition of the HM to produce a modern-day $\delta^{65}Cu_{BSE}$ – plotted as a function of the thickness of the HM. D is the sulphide-silicate Cu partition coefficient. a) Green box defines "allowed" Cu concentrations of Earth's core; $[Cu]_{core}$ < 120 ppm do not comply with the siderophile nature of Cu during core formation. Blue dotted line describes the amount of S added to the core (in wt.%) in the case of total mixing of the HM composed of a stoichiometric Fe-O-S liquid into the core. b) Lines plotted here limited to those "allowed" in top panel.

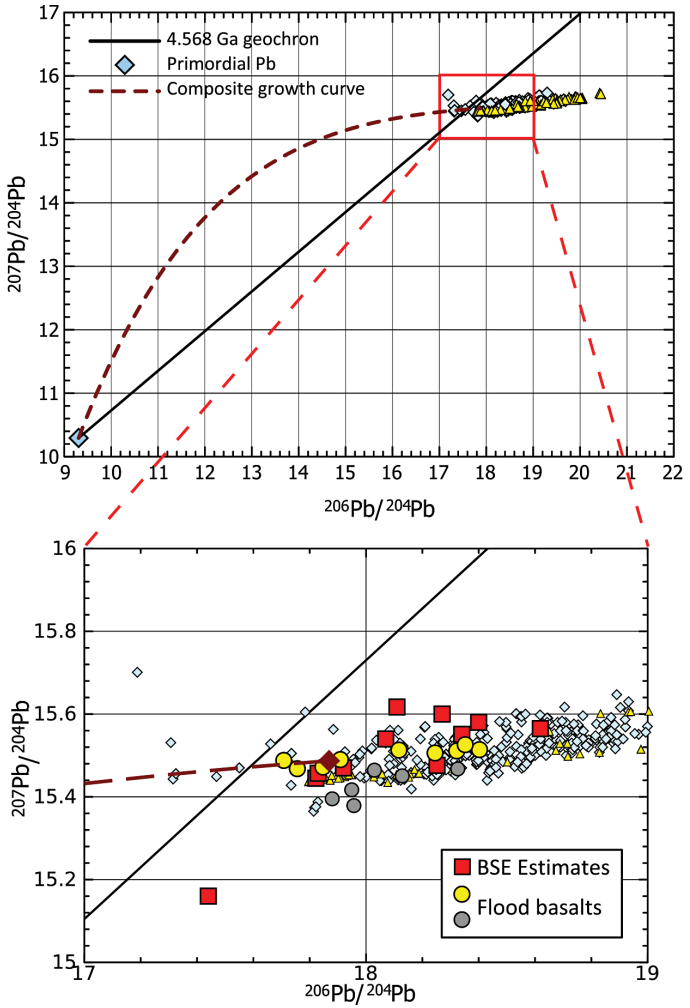

Figure 4 Modelled evolution of mantle Pb isotope composition as a result of Pb partitioning into the core at 50 Ma and the HM at 100 Ma (composite growth curve). Compilation of mid-ocean ridge basalt (MORB) and ocean island basalt (OIB) data taken from PetDB (http://www.earthchem.org/petdb) which all plot to the right (more radiogenic) side of the terrestrial (4.568 Ga) geochron (based on the evolution of Pb from primordial source – based on Canyon Diablo Troilite). Lower figure is a zoom, showing that the composite curve agrees with some of the more unradiogenic estimates for modern day BSE Pb isotope composition (Halliday, 2004), as well as the compositions of certain flood basalt provinces (yellow: Ontong Java Plateau; grey: Baffin Island) thought to best represent ancient primitive mantle composition (Jackson and Carlson, 2011).

To conclude, the Cu isotope composition of BSE seems to require that large scale sulphide-silicate equilibration occurred sometime in Earth's history; here, we have modelled it as the formation of a discreet Fe-O-S reservoir, a "Hadean Matte", which ponded to the base of the mantle during the final stages of Earth's differentiation. Such a feature likely admixed into Earth's core; however, if any of this material remains, such material could account for recently detected non-chondritic S isotope compositions in Earth's mantle (Labidi *et al.*, 2013). Finally, the Martian core is thought to have up to 14 wt. % S (Wänke and Dreibus, 1994) so FeS-silicate equilibration during core formation could have a significant effect on Mars' mantle; Cu isotopes have the potential to identify this effect.

Acknowledgements

This research was supported by the Marie Curie IOF Fellowship "Isovolc", funding from the European Research Council under the European Community's Seventh Framework Programme (FP7/2007-2013)/ERC grant agreement #207467 (DECore) and under the H2020 framework program/ERC grant agreement #637503 (Pristine), as well as the financial support of the UnivEarthS Labex program at Sorbonne Paris Cité (ANR-10-LABX-0023 and ANR-11-IDEX-0005-02). FM thanks the ANR through a chaire d'excellence Sorbonne Paris Cité and the INSU through the PNP program. ISP acknowledges support from NSF EAR0946629. The authors would like to thank Katharina Lodders, Bruce Fegley, Astrid Holzheid and Kevin Burton for discussions, Juliens Foriel and Moureau for analytical support, and Manuel Moreira, Euan Nisbet, Gary Byerly, Tim Elliott, Fang-Zhen Teng, and Rosalind Helz for sample provision. Three anonymous reviewers and executive editor Graham Pearson greatly improved the text.

Editor: Graham Pearson

Additional Information

Supplementary Information accompanies this letter at www.geochemicalperspectivesletters.org/article1506

Reprints and permission information is available online at http://www.geochemicalperspectivesletters.org/copyright-and-permissions

Cite this letter as: Savage, P.S., Moynier, F., Chen, H., Siebert, J., Badro, J., Puchtel, I.S., Shofner, G. (2015) Copper isotope evidence for large-scale sulphide fractionation during Earth's differentiation. *Geochem. Persp. Let.* 1, 53-64.

Author Contributions

P.S. and F.M. conceived the study and organised sample acquisition, F.M. and H.C. implemented the Cu isotopic analyses and improved the methods, P.S. and H.C. produced all of the Cu isotope data. P.S. produced all of the tables and figures and wrote the majority of the text. G.S., J.S. and J.B. designed and performed the high pressure experiments, performed electron probe analyses and wrote the experimental methods section. I.P. provided the komatiite samples. All of the authors were involved in critiquing the work during its authorship.

References

Albarède, F. (2009) Volatile accretion history of the terrestrial planets and dynamic implications. *Nature* 461, 1227-1233.

Arndt, N. (2008) *Komatiite*. First edition, Cambridge University Press, United Kingdom.

Badro, J., Cote, A.S., Brodholt, J.P. (2014) A seismologically consistent compositional model of Earth's core. *Proceedings of the National Academy of Science* 111, 7542-7545.

Burton, K.W., Cenki-Tok, B., Mokadem, F., Harvey, J., Gannoun, A., Alard, O., Parkinson, I.J. (2012) Unradiogenic lead in Earth's upper mantle. *Nature Geoscience* 5, 570-573.

Chen, H., Savage, P.S., Teng, F.-Z., Helz, R.T., Moynier, F. (2013) Zinc isotope fractionation during magmatic differentiation and the isotopic composition of the bulk Earth. *Earth and Planetary Science Letters* 369-370, 34-42.

Dauphas, N., Chen, J.H., Zhang, J., Papanastassiou, D.A., Davis, A.M., Travaglio, C. (2014) Calcium-48 isotopic anomalies in bulk chondrites and achondrites: Evidence for a uniform isotopic reservoir in the inner protoplanetary disk. *Earth and Planetary Science Letters* 407, 96-108.

Dreibus, G., Palme, H. (1996) Cosmochemical constraints on the sulphur content in the Earth's core. *Geochimica et Cosmochimica Acta* 60, 1125-1130.

Fitoussi, C., Bourdon, B. (2012) Silicon isotope evidence against an enstatite chondrite earth. *Science* 335, 1477-1480.

Galer, S.J.G., Goldstein S.L. (1996) Influence of accretion on lead in the Earth. In: Basu, A., Hart, S. (Eds.) *Earth Processes: Reading the Isotopic Code*, AGU Geophysical Monograph 95, 75-98.

Halliday, A.N. (2004) Mixing, volatile loss and compositional change during impact-driven accretion of the Earth. *Nature* 427, 505-509.

Herwartz, D., Pack, A., Friedrichs, B., Bischoff, A. (2014) Identification of the giant impactor Theia in lunar rocks. *Science* 344, 1146-1150.

Holzheid, A., Sylvester, P., O'Neill, H.St.C., Rubie, D.C., Palme, H. (2000) Evidence for a late chondritic veneer in the Earth's mantle from high-pressure partitioning of palladium and platinum. *Nature* 406, 396-399.

Jackson, M.G., Carlson, R. (2011) An ancient recipe for flood basalt genesis. *Nature* 476, 316-319.

Kleine, T., Palme, H., Mezger, K., Halliday, A.N. (2005) Hf-W chronometry of lunar metals and the age and early differentiation of the Moon. *Science* 310, 1671-1674.

Kramers, J.D., Tolstikhin, I.N. (1997) Two terrestrial lead isotope paradoxes, forward transport modelling, core formation and the history of the continental crust. *Chemical Geology* 139, 75-110.

Labidi, J., Cartigny, P., Moreira, M. (2013) Non-chondritic sulphur isotope composition of the terrestrial mantle. *Nature* 501, 208-211.

Lee, C.-T.A., Luffi, P., Chin, E.J., Bouchet, R., Dasgupta, R., Morton, D.M., Le Roux, V., Yin, Q.-Z., Jin, D. (2012) Copper systematics in arc magmas and implications for crust-mantle differentiation. *Science* 335, 64-66.

Lodders, K. (2003) Solar System abundances and condensation temperatures of the elements. *Astrophysical Journal Letters* 591, 1220-1247.

Luck, J.M., Ben Othman, D., Albarède., F. (2005) Zn and Cu isotopic variations in chondrites and iron meteorites: Early solar nebula reservoirs and parent-body processes. *Geochimica et Cosmochimica Acta* 69, 5351-5363.

Markl, G., Lahaye, Y., Schwinn, G. (2006) Copper isotopes as monitors of redox processes in hydrothermal mineralization. *Geochimica et Cosmochimica Acta* 70, 4215-4228.

McDonough, W.F. (2003) Compositional model for the Earth's core. In: Carlson, R.W. (Ed) *The mantle and core, Treatise on Geochemistry*,1st edition, 2, 547-568.

O'Neill, H.St.C. (1991) The origin of the moon and the early history of the earth - A chemical model. Part 2: The earth. *Geochimica et Cosmochimica Acta* 55, 1159-1172.

Palme, H., O'Neill, H.St.C. (2014) Cosmochemical estimates of mantle composition. In: Carlson, R.W. (Ed) *The mantle and core, Treatise on Geochemistry*, 2nd edition, 3, 1-39.

Poirier, J.-P. (1994) Light elements in the Earth's outer core: A critical review. *Physics of the Earth and Planetary Interiors* 85, 319-337.

Schönbächler, M., Carlson, R.W., Horan, M.F., Mock, T.D., Hauri, E.H. (2010) Heterogeneous accretion and the moderately volatile element budget of Earth. *Science* 328, 884-887.

Siebert, J., Badro, J., Antonangeli, D., Ryerson, F.J. (2013) Terrestrial accretion under oxidizing conditions. *Science* 339, 1194-1197.

Wade, J., Wood, B.J., Tuff, J. (2012) Metal–silicate partitioning of Mo and W at high pressures and temperatures: Evidence for late accretion of sulphur to the Earth. *Geochimica et Cosmochimica Acta* 85, 58-74.

Wang, Z., Becker, H. (2013) Ratios of S, Se and Te in the silicate Earth require a volatile-rich late veneer. *Nature* 499, 328-331.

Wänke, H., Dreibus, G. (1994) Chemistry and accretion history of Mars. *Philosophical Transactions of the Royal Society of London Series A* 349, 285-293.

Williams, H.M., Archer, C. (2011) Copper stable isotopes as tracers of metal-sulphide segregation and fractional crystallisation processes on iron meteorite parent bodies. *Geochimica et Cosmochimica Acta* 75, 3166-3178.

Wood, B.J., Halliday, A.N. (2005) Cooling of the Earth and core formation after the giant impact. *Nature* 437, 1345-1348.

Copper isotope evidence for large-scale sulphide fractionation during Earth's differentiation

P.S. Savage[1, 2, 3*], F. Moynier[1], H. Chen[4],
G. Shofner[1], J. Siebert[1], J. Badro[1, 5], I.S. Puchtel[6]

Supplementary Information

The Supplementary Information includes:

- Samples
- Methods for Cu isotope analysis
- Cu isotope data
- Bulk Silicate Earth and Bulk Earth Cu isotope averages
- Experimental determination of Cu isotope fractionation between metal, sulphide and silicate
- Copper isotope constraints on the thickness of the Hadean Matte
- Chemical consequences of forming the Hadean Matte on Earth's mantle and core
- Figures S-1 to S-6
- Tables S-1 to S-10
- Supplementary Information References

1. Institut de Physique du Globe de Paris, Institut Universitaire de France, Sorbonne Paris Cité – Université Paris Diderot, UMR CNRS 7154, 1 rue Jussieu, 75005 Paris, France
2. Department of Earth Sciences, Durham University, Science Labs, Durham DH1 3LE, UK
3. Department of Earth and Environmental Sciences, University of St. Andrews, Irvine Building, St. Andrews, KY16 9AL, UK
* Corresponding author: p.s.savage@dur.ac.uk
4. Department of Earth and Planetary Sciences and McDonnell Center for the Space Sciences, Washington University in St. Louis, One Brookings Drive, St. Louis, MO 63130, USA
5. Earth and Planetary Science Laboratory, Ecole Polytechnique Federale de Lausanne, CH-1015 Lausanne, Switzerland
6. Department of Geology, University of Maryland, College Park, Maryland 20742, USA

1. Samples

Choosing samples to constrain the Cu isotope composition of BSE is not trivial, due to the specific behaviour of Cu during mantle melting (Lee *et al.*, 2012). Any remaining residual sulphides will retain Cu, and partial melting with a degree typical for generating MORB or OIB magmas will not remove all Cu from a fertile peridotitic source. Such elemental fractionation could potentially give rise to isotopic fractionation. A predicted melt fraction of over 25 % is required before Cu is quantitatively transferred to the melt phase.

With this in mind, two lithologies appear suitable as prospective samples for ascertaining the copper isotopic composition of BSE. The first are komatiites, which are mantle-derived ultramafic lavas, generated by high degrees (>25 %) of mantle melting and typically found in Archaean terrains. In this study, we analysed komatiite samples from two localities; 2.4 Ga Vetreny Belt (Baltic Shield, Puchtel *et al.*, 1996) and 2.7 Ga Belingwe (South Africa; Puchtel *et al.*, 2009). The second are "fertile" orogenic lherzolites. Again, melting will deplete a mantle source, but not qualitatively so for Cu, which may give rise to isotopic fractionation. There are already Cu isotope data for peridotites, although many remain unpublished – we have used orogenic lherzolite data from such studies to use in our BSE average; specifically Lanzo (Italy; Ben Othman *et al.*, 2006) and Horoman (Japan; Ikehata and Hirata, 2012).

We analysed a number of mid-ocean ridge basalts (MORB), which are typically formed by fairly high (10-15 %) degrees of melting of upper mantle. The samples represent the major ocean basins, from the Mid-Atlantic Ridge, East Pacific Rise and Pacific Antarctic Rise, and the Central and Southwest Indian Ridges. We also include data from a variety of ocean island basalt samples to investigate the possibility of Cu isotope mantle heterogeneities. Samples were taken from a range of localities which represent a range of the posited mantle end-members (*e.g.*, Stracke *et al.*, 2005). These include Hawaii (Kilauea Iki lava lake, DMM), Iceland (Hekla volcano, DMM), Tubuaii (South Pacific, HIMU), Fogo (Cape Verde, EM-1), Santo Antao (Cape Verde, "young" HIMU), Sao Miguel (Azores, EM-2-HIMU mixture) and La Palma (Canary Islands, HIMU).

To assist in constraining a value for bulk Earth, we analysed a representative selection of enstatite chondrites (Keil, 1989). The sample set consisted of four samples from the high iron group, EH (Qingzhen EH3, Kota Kota EH3, Abee EH4 and Indarch EH4) and four from the low iron group, EL (MAC88184 EL3, LON94100 EL6, Hvittis EL6 and Eagle EL6).

2. Methods for Cu isotope analysis

All samples were received as powders, processed variously by alumina jaw crusher and disk mills, agate ball mills and mortar and pestle. Approximately 25 – 100 mg of each sample powder was dissolved in pre-cleaned PFA beakers under heat lamps, using a 4:1 mixture of concentrated, triple-distilled HF-HNO_3,

followed by 6 N HCl to destroy fluoride complexes. The HCl dissolution/dry down step was repeated, and the residues were taken up in 1 ml 7 N HCl + 0.001 % H_2O_2 for ion chromatography.

All samples and external standards were purified for Cu isotope analysis using a single column ion chromatographic technique (modified after Maréchal *et al.*, 1999). The procedure utilises Bio-Rad AG MP-1 anion resin, which, at low pH in chloride form, has a high partition coefficient for Cu. Typically, 100 % of each sample aliquot was loaded onto the column, apart from when column yield/chemistry was being tested whereby the aliquot was split 50:50 between two separate columns (see below). After sample loading, matrix elements were eluted in 7 ml of 7 N HCl + 0.001 % H_2O_2. The Cu was then eluted in a further 20 ml of 7 N HCl + 0.001 % H_2O_2. The samples were evaporated to dryness and the whole procedure was repeated to further purify the Cu. The final samples were taken up in 0.1 N HNO_3 for analysis.

Copper isotope analysis was performed on Neptune Plus Multi-Collector Inductively-Coupled-Plasma Mass-Spectrometers (MC-ICP-MS) at Washington University in St. Louis and the Institut de Physique du Globe, Paris. Samples were introduced into the instrument using an ESI PFA microflow nebuliser (100 µl min^{-1} flow rate) running into a glass spray chamber. The instrument was operated at low resolution (m/Δm ~ 450, where Δm is defined at 5 % and 95 % of peak height), with the ^{65}Cu and ^{63}Cu isotope beams collected in the C (central) and L2 Faraday cups respectively. Matrix elements were monitored using ^{62}Ni and ^{64}Zn beams in L3 and L1 in the same cup setup. Under typical running conditions, a 0.5 ppm Cu solution generated a 0.06-0.08 nA ion beam (6-8 V total signal using 10^{-11} Ω resistors). Instrument background signal (typically <10 mV total Cu) was measured at the beginning of each analytical session and the subsequent sample measurements were corrected for using these data. The total procedural blank contained ~4 ng Cu, which equates to <1 % of the Cu sample analyte.

Isotope ratios were measured in static mode, with each measurement consisting of 25 cycles of 8.4 second integrations, with a 3 second idle time. Ratios were calculated in the Thermo Neptune Data Evaluation software, which discarded any outliers at the 2 sigma confidence level. To correct for instrumental mass bias, isotope measurements were calculated using the standard-sample bracketing protocol relative to the NIST SRM976 standard, whereby variations in Cu ratios are defined using the delta notation $\delta^{65}Cu$ as follows: $\delta^{65}Cu = [(^{65}Cu/^{63}Cu_{sample} / {}^{65}Cu/^{63}Cu_{SRM976}) - 1] \times 1000$. Each sample $\delta^{65}Cu$ is an average of at least 3 analyses and a typical measurement session lasted around 12 hours. Instrumental drift over this time period was always quasi-linear. Calculating the $\delta^{65}Cu$ value of SRM976 using adjacent bracketing standard measurements for two typical analysis session gives $\delta^{65}Cu = -0.01 \pm 0.13$ ‰ (2 s.d., n = 33) and $\delta^{65}Cu = 0.00 \pm 0.05$ ‰ (2 s.d., n = 44).

To assess method accuracy and ensure inter-laboratory comparison, we routinely analysed USGS standards BHVO-2, BIR-1, BCR-2 and AGV-1/-2. Our data for these standards (Table S-1) are in excellent agreement with the accepted values. To assess method reproducibility, a number of the sample aliquots were

split 50:50; each split was separately processed through the chemistry and analysed on different days – these "repeats" are listed in Tables S-6 and S-7, and are identical to the initial measurements. A number of samples were repeated by dissolving a new aliquot of powder; again, these redissolutions have identical Cu isotope compositions to their original measurements (Tables S-1 and S-4).

Residual Na in a sample aliquot that has not been removed via the purification process can affect the accuracy of Cu isotope measurements (Larner *et al.*, 2011). Specifically, Na forms $^{23}Na^{40}Ar^+$ in the plasma of the mass spectrometer, which is nominally the same mass as $^{63}Cu^+$ and can therefore result in an overestimate of this isotope, driving the measured Cu isotope ratio to artificially lighter values. The ion chromatography procedure described above should quantitatively remove Na; nevertheless, we tested the magnitude of such an effect by doping aliquots of the Cu bracketing standard (SRM987, 250 ppb Cu) with various quantities of Na, resulting in Na/Cu values in the standards ranging from 0.001 to 1. Analysis of these aliquots shows that increasing Na/Cu results in an isotopic shift to lighter values, as predicted (Table S-1, Fig. S-1), with an offset of ~0.1 ‰ at high (>0.4) Na/Cu values. However, at lower Na/Cu this effect is minor, and does not result in an isotopic shift within error, from the standard. As a matter of course, we monitored the Na/Cu of each sample before analysis – if greater than 0.1, further sample purification was performed. With most of the mafic and ultramafic samples analysed for this study, low Na contents means that this is rarely an issue. Nevertheless, the presence of Na (coupled with low Cu contents) in a sample has the potential to bias Cu isotope data, and we were very careful to monitor sample [Na].

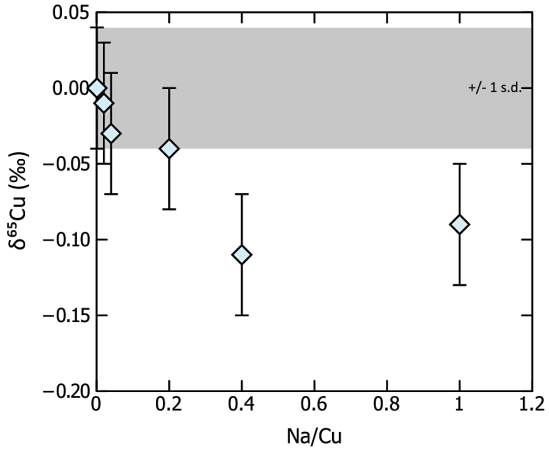

Figure S-1 Results of Na doping tests on Cu isotope measurements – sample is 250 ppb Cu SRM976 doped with various Na concentrations to results in Na/Cu between 0.001 and 1. Measurable isotopic offsets are present in samples with Na/Cu values of >0.2. Error bars are 1 s.d.

Table S-1 Cu isotope standards.

Sample	δ^{65}Cu (‰)	2 s.d.	n	Ref
BHVO-2	0.14	0.05	5	
	0.06	0.01	3	
	0.11	0.02	3	
Average	**0.10**	**0.08**	**3**	
	0.10	0.04		Moeller *et al.*, 2012
	0.10	0.07		Moynier *et al.*, 2010
	0.15	0.05		Liu *et al.*, 2014
AGV-1	-0.01	0.03	4	
	-0.01	0.09	3	
AGV-2	0.01	0.11	3	
Average	**0.00**	**0.02**	**3**	
	0.11	0.04		Moeller *et al.*, 2012
	0.10	0.11		Moynier *et al.*, 2010
	0.05	0.04		Liu *et al.*, 2014
BIR-1	0.09	0.01	2	
	0.08	0.07		Moeller *et al.*, 2012
	-0.02	0.1		Li *et al.*, 2009
	-0.01	0.04		Liu *et al.*, 2014
BCR-2	0.19	0.07	2	
	0.14	0.05		Moeller *et al.*, 2012
	0.07	0.08		Archer and Vance, 2004
	0.19	0.08		Bigalke *et al.*, 2010
	0.22	0.04		Liu *et al.*, 2014
Na doping tests				
Sample	**δ^{65}Cu (‰)**	**2 s.d.**	**Na/Cu**	
Cu SRM976 (250 ppb Cu)	0.00	0.08	0.001	
SRM976 + 5 ppb Na	-0.01	0.08	0.02	
SRM976 + 10 ppb Na	-0.03	0.08	0.04	
SRM976 + 50 ppb Na	-0.04	0.08	0.2	
SRM976 + 100 ppb Na	-0.11	0.08	0.4	
SRM976 + 250 ppb Na	-0.09	0.08	1	

3. Cu isotope data

Terrestrial sample Cu isotope data used in calculating $\delta^{65}Cu_{BSE}$ are presented in Tables S-2 thru S-7, and the enstatite chondrite data are given in Table S-8.

Komatiite Cu isotope data are presented in Table S-2. The Vetreny and Belingwe komatiites have Cu contents equal or greater than those predicted by melting of a fertile mantle source (Lee *et al.*, 2012), hence we use these sample data to provide a komatiitic Cu isotope average of δ^{65}Cu = 0.06 ± 0.06 ‰ (2 s.d., n = 14).

We use the lherzolite literature data from two sources (Ben Othman *et al.*, 2006; Ikehata and Hirata, 2012). Ben Othman *et al.* (2006) analysed the Cu isotope ratio of peridotites from two massifs, Beni-Bousera and Lanzo and three xenolith suites, Kilbourne Hole, San Carlos and Kaapvaal. All data describe a fairly wide spread (δ^{65}Cu = –0.22 to 0.15 ‰), however, only the Lanzo suite were samples of orogenic lherzolites, and these define a much narrower isotopic range. It is these data we utilise in our BSE average (Table S-3); average δ^{65}Cu = 0.08 ± 0.12 ‰ (2 s.d., n = 9).

Ikehata and Hirata (2012) utilised laser ablation MC-ICP-MS to analyse native Cu grains from orogenic lherzolites from the Horoman massif, Japan. Morphologically, the Cu grains were identified as either primary (magmatic) or secondary (metasomatic). The primary Cu grains have a very limited Cu isotope range (δ^{65}Cu = 0.04 to 0.07 ‰, Table S-3), and are identical to a plagioclase lherzolite the same study analysed by solution MC-ICPMS. These data give an average value of δ^{65}Cu = 0.05 ± 0.02 ‰ (2 s.d., n = 7).

To investigate possible Cu isotope heterogeneities in the mantle, as well as the possibility of Cu isotope fractionation during different degrees of partial melting, a comprehensive selection of mid-ocean ridge basalts (MORBs) and ocean island basalts (OIB) with varying chemical affinities were analysed (see SI Section 1). The MORB data are given in Table S-4. The data span a very narrow range (δ^{65}Cu = 0.00 to 0.12 ‰) and there are no variations between ocean basins, hence we take a global MORB average of δ^{65}Cu = 0.06 ± 0.06 ‰ (2 s.d., n = 17).

The OIB data are given in Tables S-5 thru S-7. These included two suites of basalts from "depleted mantle"-type plumes (Kilauea Iki lava lake, Hawaii and Hekla volcano, Iceland), as well as more isotopically "enriched" end-member plumes: Tubuaii, South Pacific, (HIMU), Fogo, Cape Verde (EM-1), Santo Antao, Cape Verde ("young" HIMU), Sao Miguel, Azores (EM-2-HIMU mixture) and La Palma, Canary Islands (HIMU).

Cu isotope analysis of 2 eruption samples and 8 Kilauea Iki lava lake samples reveal little variation (Table S-4). The average composition of Kilauea Iki lavas is δ^{65}Cu = 0.04 ± 0.09 ‰ (2 s.d., n = 10; Table S-5). The average value for Hekla basalts, δ^{65}Cu = 0.08 ± 0.13 ‰ (2 s.d., n = 5; Table S-6) is identical to Kilauea Iki (as well as the komatiite, MORB and lherzolite values). The final ocean island basalts (OIBs) representing various mantle isotopic "end-members" (Stracke *et al.*, 2005) are less well-characterised than the others described above,

with scant elemental data available in the literature. Nevertheless, the range of Cu isotope compositions defined by the OIBs is slightly larger, but generally comparable to the other datasets (δ^{65}Cu range = –0.07 to 0.16 ‰, Table S-7) and the average value (δ^{65}Cu = 0.07 ± 0.14 ‰ 2 s.d., n = 15) is identical to all the others described above.

Our new data for the enstatite chondrites are given in Table S-8. The group averages for EH and EL chondrites (EH δ^{65}Cu = –0.23 ± 0.06 ‰; EL δ^{65}Cu = –0.26 ± 0.13 ‰) are notable in that they are isotopically indistinguishable from each other but are distinct from all other chondrite groups (see Fig. 1 in main text).

Table S-2 Komatiites.

Sample	δ^{65}Cu (‰)	2 s.d.[1]	n	Age (Ga)	Cu (ppm)
Vetreny					
91105/1	0.10	0.05	3	2.40	63
91105	0.04	0.07	3	2.40	54
91104	0.04	0.09	3	2.40	67
91106	0.04	0.01	3	2.40	62
12101	0.05	0.01	5	2.40	95
12111	0.10	0.02	5	2.40	94
12117	0.00	0.07	5	2.40	92
12124	0.09	0.02	5	2.40	95
Belingwe					
TN1	0.06	0.01	5	2.69	67
TN3	0.03	0.02	5	2.69	75
TN16	0.06	0.02	5	2.69	47
TN17	0.03	0.02	3	2.69	51[2]
TN21	0.11	0.02	5	2.69	45[2]
ZV10	0.07	0.02	3	2.69	52
Average	**0.06**	**0.06**	**14**		

[1] 2 standard deviations based on either the repeat measurements or, in the case where there is only 1 measurement, based on the 2 s.d. of external standard analysis that day.
[2] Cu concentrations measured on MC-ICP-MS at Washington University in St. Louis.

Table S-3 Peridotites (orogenic lherzolites - literature).

Lanzo	δ^{65}Cu (‰)	2 s.d.	n
Ben Othman *et al.*, 2006	-0.01		
	0.13		
	0.01		
	0.03		
	0.09		
	0.09		
	0.15		
	0.10		
	0.15		
Average	**0.08**	**0.12**	**9**
Horoman			
Type 1 (magmatic native Cu), Ikehata and Hirata, 2012	0.04		
	0.06		
	0.07		
	0.06		
	0.04		
	0.05		
Plagioclase lherzolite, Ikehata and Hirata, 2012	0.05		
Average	**0.05**	**0.02**	**7**

Table S-4 Mid ocean ridge basalts.

Sample	δ^{65}Cu (‰)	2 s.d.	n
Mid Atlantic Ridge			
DIVA1 15-5	0.09	0.03	3
DIVA1 13-3	0.09	0.03	3
EW9309 27D-1g	0.12	0.05	3
EW9309 4D-3g	0.06	0.01	3
EW9309 10D-3g	0.07	0.04	3
RD87 DR29-101	0.06	0.05	3
RD87 DR24	0.02	0.02	3
RD87 DR18-102	0.06	0.03	3
Central Indian Ridge			
MD57 D7-5	0.04	0.01	3
MD57 D2-8	0.04	0.09	3
Pacific Antarctic Ridge			
PAC2 DR37-3g	0.08	0.01	3
PAC2 DR32-1g	0.08	0.02	3
East Pacific Rise			
SEARISE2 DR3	0.04	0.00	3
redissolution	0.05	0.03	3
CYP78 12-34	0.07	0.04	3
Southwest Indian Ridge			
SWIFT DR32-1-3g	0.10	0.02	3
SWIFT DR06-3-6g	0.06	0.05	3
SWIFT DR04-2-3g	0.00	0.03	3
Average	**0.06**	**0.06**	**17**

Table S-5 Kilauea Iki.

Sample	δ^{65}Cu (‰)	2 s.d.[1]	n	Cu (ppm)	MgO (wt.%)
Eruption samples					
Iki-22	0.06	0.08	1	120	19.52
Iki-58	0.06	0.08	1	124	8.08
Lava lake					
KI67-3-6.8	0.08	0.08	1	60	25.83
KI79-3-150.4	-0.02	0.08	1	102	13.51
KI67-3-27.5	0.04	0.08	1	86	12.01
KI75-1-121.5	0.14	0.08	1	138	7.77
KI75-1-75.2	-0.01	0.08	1	168	5.77
KI79-1R1-170.9	0.00	0.08	1	365	3.48
KI67-2-85.7	0.05	0.08	1	450	2.6
KI81-2-88.6	0.04	0.08	1	345	2.37
Average	**0.04**	**0.09**	**10**		

[1] Errors based on the 2 s.d. of external standard analysis that day.

Table S-6 Hekla.

Sample	δ^{65}Cu (‰)	2 s.d.[1]	n	Cu (ppm)	SiO_2 (wt. %)
Basalts					
HEK04-09	0.14	0.08	1	39.8	46.97
HEK05-09	0.00	0.08	1	47.1	46.47
repeat	0.01	0.21	2		
HEK09-09	0.06	0.08	1	47.3	46.64
repeat	-0.02	0.10	3		
HEK07-09	0.11	0.08	1	25.4	47.01
HEK12-09	0.13	0.08	1	26	46.42
Average	**0.08**	**0.13**	**5**		

[1] 2 standard deviations based on either the repeat measurements or, in the case where there is only 1 measurement, based on the 2 s.d. of external standard analysis that day.

Table S-7 Ocean island basalts.

Sample	δ^{65}Cu (‰)	2 s.d.[1]	n
Santo Antao			
SA-1	0.12	0.09	1
SA-5	0.00	0.05	2
repeat	-0.06	0.03	3
SA-6	0.10	0.07	2
SA-8	0.12	0.09	1
SA-11	-0.07	0.05	2
repeat	-0.07	0.07	3
La Palma			
W-1949 48c	0.16	0.10	2
1585 45d	0.13	0.09	1
LP69d	0.08	0.03	2
repeat	0.03	0.04	3
Sao Miguel			
SM-7	0.08	0.09	1
repeat	0.03	0.11	3
SM-33	0.02	0.07	2
Fogo			
FG-2	0.11	0.00	2
FG-6	0.12	0.10	2
repeat	0.08	0.06	3
FG-12	0.14	0.09	1
Tubuaii			
TBA-C29	0.02	0.07	2
Iceland			
RHY01-09	-0.03	0.09	1
Average	**0.07**	**0.14**	**15**

"Repeat" signifies reanalysis of the same sample aliquot on a different day.
[1] 2 standard deviations based on either the repeat measurements or, in the case where there is only 1 measurement, based on the 2 s.d. of external standard analysis that day.

Table S-8 Enstatite chondrites.

Sample	Type	δ^{65}Cu (‰)	2 s.d.[1]	n
EH				
Qingzhen	EH3	-0.29	0.03	3
Kota Kota	EH3	-0.15	0.03	3
Abee	EH4	-0.24	0.06	3
Indarch	EH4	-0.25	0.05	3
Average EH		**-0.23**	**0.06**	**4**
EL				
MAC88184	EL3	-0.11	0.06	3
LON94100	EL6	-0.21	0.03	3
Hvittis	EL6	-0.38	0.03	3
Eagle	EL6	-0.35	0.05	3
Average EL		**-0.26**	**0.13**	**4**

4. Bulk Silicate Earth and Bulk Earth Cu isotope averages

The average Cu isotope compositions for all the terrestrial samples analysed in this study, as well as the literature data for peridotites, are summarised in Table S-9 and in Figure 1 and Figure S-2. Also listed is the average value of various basaltic standards given by the literature data (see Table S-1). As all averages are statistically identical and the distribution of all data is normal, a simple arithmetic mean is taken for the BSE value, which gives a composition of δ^{65}Cu = 0.07 ± 0.10 ‰ (2 s.d.).

The Cu isotope compositions of all chondrite groups are presented in Table S-9, as well as the average Cu content for each group (Luck *et al.*, 2003, 2005; Barrat *et al.*, 2012). The Chondritic Bulk Earth (CBE) was calculated by using the "best" mixture of ordinary and carbonaceous chondrites estimated in Fitoussi and Bourdon (2012) for the Earth, using O and Cr isotopes (0.16 CI: 0.21 CO: 0.63 LL), which, when weighted using [Cu], gives a value of $\delta^{65}Cu_{CBE}$ = −0.19 ± 0.10 ‰, 2 s.d. Another estimate, made using a chondritic mixture based on O isotopes as well as major element considerations (given by Lodders, 2000, as 0.70:0.21:0.05:0.04 EH:H:CV:CI), results in a bulk Earth composition of δ^{65}Cu = −0.28 ± 0.07 ‰, 2 s.d.

Using a mixture of 50:50 EH:EL chondrites gives an Enstatite Chondrite Bulk Earth (ECBE) value of $\delta^{65}Cu_{ECBE}$ = −0.24 ± 0.09 ‰, 2 s.d., statistically identical to that of $\delta^{65}Cu_{CBE}$. This would also be the value for BSE assuming that as

Cu is a moderately volatile element, the majority of Cu in the mantle was delivered late on in Earth's accretion, mostly from the giant impactor. This is because the most recent estimate of the impactor composition, based on high precision O isotope measurements, suggests that it was, isotopically, closest to enstatite chondrites (Herwartz *et al.*, 2014). Of all the estimates for bulk Earth calculated from chondrites, we conservatively utilise the closest value to that of the mantle in the following modelling ($\delta^{65}Cu_{CBE}$ = −0.19 ± 0.10 ‰).

Table S-9 BSE and bulk Earth averages.

BSE average Group	Average δ^{65}Cu (‰)	2 s.d.	n	
Komatiites	0.05	0.06	14	
Orogenic lherzolites	0.07	0.09	16	
MORBs	0.06	0.06	17	
Kilauea Iki basalts	0.04	0.09	10	
Hekla basalts	0.08	0.13	5	
OIBs	0.07	0.14	15	
Basaltic standards	0.06	0.11	3	
BSE average	**0.07**	**0.10**	**80**	
Bulk Earth average Meteorite group	**Average δ^{65}Cu (‰)**	**2 s.d.**	**n**	**Average Cu (ppm)**
CI	0.02	0.16	3	122
CM	-0.50	0.06	2	115
CO	-0.86	0.07	2	122
CV	-1.45	0.08	2	100
H	-0.44	0.11	3	81
L	-0.08	0.13	5	88
LL	0.07	0.06	2	80
EH	-0.23	0.06	4	210
EL	-0.26	0.13	4	120
CBE average	**-0.19**	**0.10**		
ECBE average	**-0.24**	**0.09**		
ACBE average	**-0.28**	**0.07**		

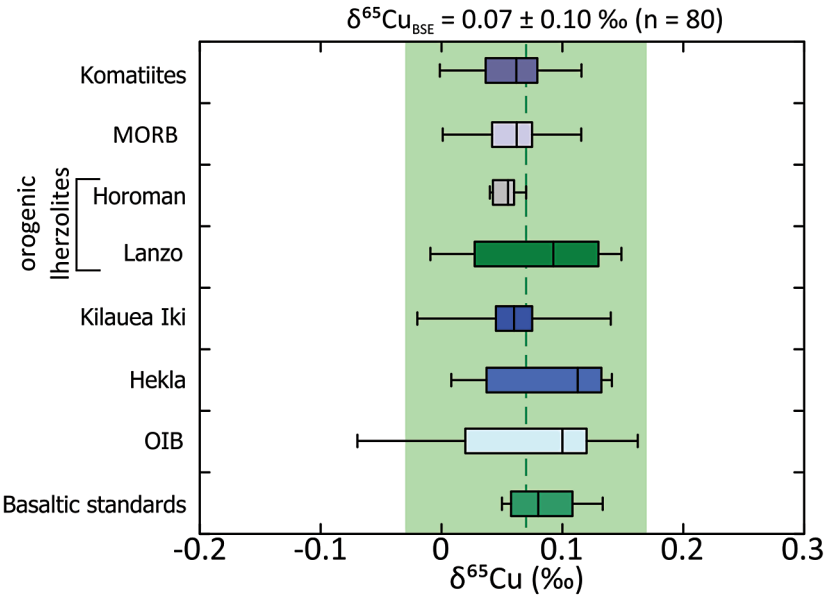

Figure S-2 Box and whisker plot showing the range of Cu isotope compositions for the terrestrial samples used in constraining the BSE Cu isotope composition. Box represents 1st and 3rd quartile, line in box represents the median and "whiskers" show the range of the data (see Tables S-2-S-7, S-9). There is no statistical difference between each group. Calculated BSE value plotted as green dashed line, green box shows 2 s.d. precision of the estimate.

5. Experimental determination of Cu isotope fractionation between metal, sulphide and silicate

The following represents a pilot study to confirm the sense and approximate magnitude of equilibrium Cu isotope fractionation that results from high temperature, high pressure equilibration of Cu between metal, silicate, and sulphide phases. Only temperature was varied.

Experiments were performed at 2 GPa at temperatures between 1400 and 1750 °C using an end-loaded piston cylinder apparatus at IPG, Paris. All experiments were conducted using a standard talc/Pyrex (below 1550 °C) or $BaCO_3$ (above 1550 °C) pressure cell, graphite furnace, inner MgO spacers, and 8 mm diameter MgO capsules with 3 mm diameter sample chambers (Siebert *et al.*, 2011). Oxygen fugacity was kept <IW –1 such that Cu should have a 1+ valence. Temperature was monitored using a type D thermocouple ($W_{97}Re_3/W_{75}Re_{25}$) inserted axially in an alumina four-bore thermocouple sleeve above the capsule. Temperature uncertainties are estimated as less than ± 25 °C for all runs. Thermal gradients can generate isotopic fractionation through thermal diffusion of heavier

isotopes in the colder region of the samples. However, the difference in average temperatures between metal and silicate liquids are likely to be much smaller than 25 °C as the two phases are distributed over the entire thermal gradient of the capsule. Samples were first taken to run pressure before quickly ramping (100-200 °C/min) to run temperatures at superliquidus conditions. Temperatures for the sulphide experiments were typically lower, because of the lower melting point of FeS at 2 GPa compared to pure Fe metal.

Experiments were quenched by turning off the electrical power to the furnace. Run duration was kept short (~1 min for metal-silicate experiments, ~5 min for sulphide-silicate, Table S-10) to avoid percolation of the charge through the polycrystalline MgO capsules and limit MgO contamination (it has been shown that run durations as short as few tens of second, at superliquidus conditions, were sufficient to reach chemical equilibrium at similar P–T conditions; Thibault and Walter, 1995). Moreover, similar run durations were found sufficient to reach Fe isotope equilibrium (Poitrasson *et al.*, 2013), albeit at higher temperatures. Starting materials were prepared by mixing powders of metallic Fe or FeS with ground natural MORB. Relative proportions of metal/sulphide and silicate were 1/3 and 2/3 by mass respectively for all experiments. Cu was added at the 1 wt. % level as high purity CuO oxide, Cu metal or a 50:50 mixture of the two to assess isotopic equilibration with "reversal experiments" (see Table S-10 for details).

Elemental data was acquired via electron microprobe, carried out with a Cameca SX100. Due to the quench textures, analyses with a 20 µm defocused beam for both metal and silicate melts were used to determine the bulk compositions. Operating conditions were 15 kV accelerating voltage, 10 nA beam current and counting times of 10–20 s on peak and background for major elements in silicate (Si, Mg, Fe, Al, Ca, Na, Ti) and metal (Fe, S, Cu, O). Multiple analyses of all phases revealed only minor chemical variations, indicating homogeneous phase composition and confirming that chemical equilibrium had been reached.

Experimental charges were separated from their capsule and, in the case of the metal-silicate experiments, ground to a fine powder in an agate pestle and mortar. The magnetic phase was separated using a hand magnet and dissolved in conc. HCl, which further avoided digestion of silicate material. The remaining silicate powder was dissolved as for the rest of the silicate samples. Note that this will not guarantee quantitative separation, so the fractionation factors listed below are likely to be minimum values.

For the sulphide-silicate experiments, much of the sulphide coalesced into a ball, which was picked from the charge (given the sulphide started as a disseminated powder, this is further evidence that the charges were well equilibrated – a similar fact is true for the metal-silicate experiments whereby all the Cu was added as CuO – and no CuO was detected after the experiment had run). This was then digested in aqua regia overnight. Imaging of these charges revealed a significant amount of disseminated sulphides in the silicate phase; presence of such in the silicate dissolution will overwhelm the silicate Cu isotope signature,

given the extremely high Cu content in all sulphides. To date, efforts to remove the sulphides by leaching have been unsuccessful. Therefore, we analysed the sulphide bleb against the starting Cu metal which, assuming no Cu loss (see below), gives a qualitative sense of Cu isotope fractionation – sufficient for our modelling. Efforts to further constrain Cu isotope behaviour in this respect are ongoing. All experiment dissolutions were purified by column chemistry and analysed as for natural samples (see SI Section 2).

The results of the piston cylinder experiments are given in Table S-10. For the metal-silicate experiments, using the partition coefficient parameterisation given in (Corgne *et al.*, 2008) predicts $D^{Cu}_{metal\text{-}silicate}$ values of between 35 and 45. The predicted and measured $D^{Cu}_{metal\text{-}silicate}$ values are within the same magnitude and the experimental values show a general increase with increasing temperature – an exception being experiment 61. This was repeated (experiment 73) and a more realistic $D^{Cu}_{metal\text{-}silicate}$ value was measured – the high D value measured in experiment 61 is thought to be a result of $BaCO_3$ contamination in the charge. To confirm equilibrium was reached in the experiments, a reversal experiment (71, 72 and 73) was performed – the $D^{Cu}_{metal\text{-}silicate}$ values and $\Delta^{65}Cu$ values are identical, implying equilibrium was reached. Further evidence for the lack of Cu loss during these experiments comes from calculating the bulk Cu isotope composition of the charge based on phase compositions (*i.e.* metal + silicate) and comparing it to the composition of the bulk experiment, *i.e.* that of the CuO (or Cu metal) added to the charge, which are equal (calculated av. $\delta^{65}Cu = 0.16 \pm 0.02$ ‰ vs. CuO $\delta^{65}Cu = 0.15 \pm 0.02$ ‰; when Cu was added as Cu metal: calculated $\delta^{65}Cu = 0.13 \pm 0.05$ ‰ vs. Cu metal $\delta^{65}Cu = 0.13 \pm 0.03$ ‰; see Table S-10). Note that there was one aliquot of CuO powder used during the experiments that was exhausted before we could analyse its bulk composition (exp. 71 and 73) and these bulk compositions are slightly different to the others. Although we could not perform such tests with our sulphide experiments, we are confident that, given the similar experimental conditions, lower experimental temperatures, homogeneous phase compositions etc., no Cu was lost from those charges either.

For the sulphide experiments, Cu contents in the silicates were typically below regular detection limits of the instrument (<200 ppm Cu); however, these concentrations can give us order of magnitude estimates on $D^{Cu}_{sulfide\text{-}silicate}$ ranging between 500 and 900. These are in line with estimates based on more detailed studies (Gaetani and Grove, 1997; Fellows and Canil, 2012); this, along with lack of elemental zoning seen in the electron probe analyses, indicates that chemical equilibrium was met. In all piston-cylinder experiments, there is some reaction of the charge with the capsule material (in our case, MgO). Typically, Fe will react with MgO to form ferro-periclase; in this case, Fe is removed from the charge. If large amounts of Fe are lost, then FeS will not be stable, and other non-stoichiometric sulphide phases may form, potentially affecting Cu (isotope) partitioning. In our case, we kept the experimental run times as short as possible to avoid this, nevertheless, the MgO content of our charge increased slightly, indicating capsule interaction. To check for this, we measured sulphide Fe and

S concentrations by electron microprobe; in all cases, the sulphide has equal molar amounts of Fe and S (1:1) indicating that the sulphide phase was FeS, and suggesting that the degree of Fe loss did not affect S activity.

All metal-silicate experiments give positive $\Delta^{65}Cu_{met\text{-}sil}$ (where $\Delta^{65}Cu_{x\text{-}y} = \delta^{65}Cu_x - \delta^{65}Cu_y$, Table S-10) in that the metal phase is consistently enriched in the heavier Cu isotope. The data agree with the sense and general magnitude of the $\Delta^{65}Cu_{met\text{-}sil}$ value measured in Williams and Archer (2011), viz. +0.48 ‰, on the basis of one analysis of a silicate-bearing iron meteorite. There does not appear to be a strong control of temperature over $\Delta^{65}Cu_{met\text{-}sil}$ (Fig. S-3) over the T range used in the experiments. As a result, we cannot parameterise the fractionation factor as a function of temperature to predict the $\Delta^{65}Cu_{met\text{-}sil}$ value at temperatures associated with core formation, except to say that, as temperatures increase, equilibrium isotope fractionation factors approach unity. Hence, these are certainly maximum values in terms of temperature dependence; however, they are also potentially minimum values given that we could not be sure that complete phase separation was achieved during processing. Also we do not have any data on how parameters such as pressure, oxygen fugacity and composition affect the fractionation factor, which could equally cause the $\Delta^{65}Cu_{sil\text{-}met}$ to increase in magnitude. Clearly, further studies are necessary.

As noted above, we were unable to quantitatively remove sulphides from the "silicate" phases of the experiments. Instead we have analysed the sulphide bleb as well as the Cu starting material, in an effort to constrain the sense (and order of magnitude) of Cu isotope fractionation during sulphide-silicate equilibrium – this is assuming minimal Cu loss, which we believe is valid (see above). In both experiments, the sulphide was enriched in the lighter Cu isotope relative to the bulk and, also, isotopic difference is smaller at higher temperatures (Table S-10, Fig. S-4), indicating that $\Delta^{65}Cu_{sulfide\text{-}sil}$ is negative and reduces with temperature, as would be predicted. Using mass balance to estimate order-of-magnitude $\Delta^{65}Cu_{sulfide\text{-}sil}$ values gives a wide range, from ~ –0.5 to –20‰, due to the large effect of error propagation. In light of the higher temperatures of core formation relative to these experiments, as well as the degree of fractionation observed previously in secondary sulphide minerals (viz. > –3.0 ‰; Markl *et al.*, 2006), we tentatively suggest that lower magnitudes in the range predicted by our experiments (*e.g.*, $\Delta^{65}Cu_{sulfide\text{-}sil} > -1.0$ ‰) are more likely.

6. Copper isotope constraints on the thickness of the Hadean Matte

Our model for the formation of a Fe-O-S layer at the base of Earth's mantle, *i.e.* the Hadean Matte, is based on O'Neill (1991) and Lee *et al.*, (2007), whereby such a layer forms as the last liquid remaining after crystallisation of a magma ocean. At that time, the core was 99 % of its present size. The Fe-O-S layer is denser than the silicate mantle, and so it sinks to the core-mantle boundary. There is no limit as to whether it is subsequently admixed into the core, but re-equilibration with the mantle should be limited. In the model, we do not take into account any additional Cu added to Earth via late veneer, as it should be volumetrically

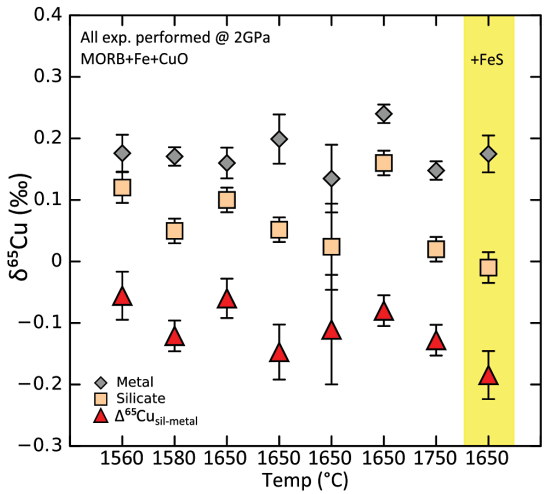

Figure S-3 Summary of metal-silicate Cu isotope equilibration experiments – note that this figure is not a graph (the x axis is discrete, not continuous). All $\Delta^{65}Cu_{sil\text{-}met}$ values are negative but there does not appear to be a strong temperature control on these values. The one experiment with S added gives the largest $\Delta^{65}Cu_{sil\text{-}met}$ value, this makes sense if there is minor amounts of S-hosted Cu that was dissolved with the non-magnetic ("silicate") phase – as Cu sulphides are shown to be isotopically light w.r.t. silicates and metal. Error bars are 1s.d.

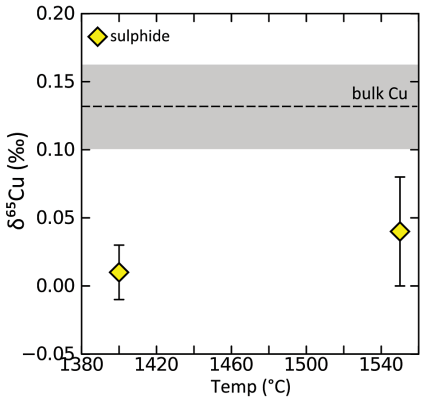

Figure S-4 Summary of sulphide-silicate Cu isotope equilibration experiments – we are so far unable to successfully measure the silicate phase, due to the presence of disseminated sulphides which overwhelm the Cu isotope signature of the silicates. Here we show the Cu isotope composition of the bulk Cu metal as well as sulphide phases from two experiments (wherein only the temperature was varied). In both cases the sulphides are enriched in the light Cu isotope relative to bulk, and there is a small decrease in fractionation magnitude (although within error) as temperature increases.

Table S-10 Experimental results.

Metal-silicate experiments		All @ 2 GPa							
Initial components: MORB + Fe + CuO									
Experiment	**Phase**	**δ^{65}Cu (‰)**	**2 s.d.**	**Cu conc.**	**D $[Cu]_m/[Cu]_{sil}$**	**Δm-sil (‰)**	**2 s.d.**	**T °C**	**t @ max T**
61	Silicate	0.10	0.04	238 ppm	160	0.06	0.06	1650	1 min
	Metal	0.16	0.05	3.8 %					
67	Silicate	0.05	0.04	484 ppm	38	0.12	0.05	1580	1 m 20 s
	Metal	0.17	0.03	1.9 %					
68	Silicate	0.12	0.05	441 ppm	49	0.06	0.08	1560	30 s
	Metal	0.18	0.06	2.1 %					
69	Silicate	0.02	0.04	432 ppm	58	0.13	0.05	1750	30 s
	Metal	0.15	0.03	2.5 %					
Reversal experiments									
Initial components: MORB + Fe + Cu + CuO									
71	Silicate	0.05	0.04	668 ppm	64	0.15	0.09	1650	35 s
	Metal	0.20	0.08	4.3 %					
Initial components: MORB + Fe + Cu									
72	Silicate	0.02	0.04	478 ppm	69	0.11	0.07	1650	30 s
	Metal	0.13	0.06	3.3 %					
Initial components: MORB + Fe + CuO									
73	Silicate	0.16	0.04	507 ppm	54	0.07	0.05	1650	30 s
	Metal	0.24	0.03	2.8 %					
Initial components: MORB + Fe + CuO + FeS									
64	Silicate	-0.01	0.05		46	0.18	0.08	1650	30 s
	Metal	0.17	0.06						
Initial components: MORB + FeS + Cu					D $[Cu]_{sul}/[Cu]_{sil}$	Δsul-bulk (‰)			
ELMO113	Silicate	n/a		~50ppm	~500	-0.12	0.04	1400	6 min
	Sulphide	0.01	0.02	2.6 %					
ELMO114	Silicate	n/a		~60ppm	~900	-0.09	0.05	1550	3 min
	Sulphide	0.04	0.04	5.4%					
Bulk Cu	**Metal**	**0.13**	**0.03**	**99.99%**					
Bulk CuO	**Oxide (CuO)**	**0.15**	**0.02**	**~80%**					

Experiments 71 and 72 are reversal experiments (i.e. all Cu in 72 was reduced, all Cu in 71 was CuO). Experiment 73: repeat of Experiment 61 – high D value due to $BaCO_3$?

insignificant relative to the amount of Cu left in the mantle. In terms of Cu, this means that the current BSE evolved over a two stage process, where first Cu was sequestered into the core, and then into the Fe-O-S layer – with the attendant isotopic fractionation associated with each phase equilibration.

The first issue when attempting a Cu isotope mass balance is to fix the abundances of Cu in the BSE, the bulk Earth, and the core. McDonough (2003) gives 30 ppm as an estimate for BSE, based on the Cu vs. MgO correlation of massif peridotites. However, Palme and O'Neill (2014) suggest that 30 ppm Cu in the BSE is too high, and use the average composition of xenolith peridotites (20 ppm Cu) as a more realistic estimate. Corgne *et al.* (2008) also suggested that 20 ppm BSE Cu is a more realistic estimate, based on partitioning experiments. These data suggest that the core should have ~ 160 ppm Cu, which translates into 64 ppm Cu in the bulk Earth. Hence, we take these estimates (BSE = 20 ppm, bulk Earth = 64 ppm, core = 160 ppm) as working abundances for our mass balance.

Assuming the Fe-O-S layer (hereafter referred to as "HM", Hadean Matte) forms as a constant thickness mantling the core, then its mass (m_{HM} in kg) can be related to its thickness (x_{HM} in m) by:

$$m_{HM} = \frac{4}{3}\pi\rho\left[\left(x_{HM} - r_{core}\right)^3 - \left(r_{core}\right)^3\right] \qquad \text{[Eq. S-1]}$$

where ρ is the assumed density of a Fe-O-S liquid (7000 kg m^{-3}) and r_{core} is the radius of the core (3.47 x 10^6 m). The mass of Cu in the HM (m_{HM}^{Cu}) can then be estimated using the partition coefficient ($D^{Cu}_{S\text{-}Sil}$) of Cu between sulphide and silicate liquid such that:

$$m_{HM}^{Cu} = D_{S-sil}^{Cu} \times [Cu]_{BSE} \times m_{HM} \qquad \text{[Eq. S-2]}$$

where $[Cu]_{BSE}$ is the current Cu concentration of Bulk Silicate Earth (20 ppm). Values of $D^{Cu}_{S\text{-}Sil}$ between silicate and sulphide liquids have been experimentally determined, and can exceed 1000 (Gaetani and Grove, 1997; Fellows and Canil, 2012; Kiseeva and Wood, 2013). However, the presence of O in a FeS liquid will reduce the chalcophile nature of Cu (Kiseeva and Wood, 2013), and recent work suggests that Cu is more compatible in silicate phases than earlier estimates predicted. As such, we have limited the $D^{Cu}_{S\text{-}Sil}$ values in our model to between 100 and 500.

We then use the estimated concentration of Cu in the core (160 ppm) and apportion this reservoir between the core and HM. This model thus provides an adjusted Cu composition of the core by:

$$[Cu]_{core} = \frac{[Cu]_m - f_{HM}^{Cu} \cdot [Cu]_{HM}}{\left(1 - f_{HM}^{Cu}\right)} \qquad \text{[Eq. S-3]}$$

where $[Cu]_m$ is the total Cu (160 ppm) and f^{Cu}_{HM} is the fraction of Cu in the Hadean Matte, where $f^{Cu}_{HM} = m^{Cu}_{HM} / (m^{Cu}_{HM} + m^{Cu}_{core})$. Equations S-1, S-2

and S-3 can be combined to relate $[Cu]_{core}$ to x_{HM}, the results for $D^{Cu}_{S\text{-}Sil}$ values of 100, 200, and 500 are shown in Figure 3a in the main text.

Further constraints can be placed on this model. Although Cu becomes less siderophile at high pressures associated with magma ocean fractionation, the metal phase should be enriched by at least a factor of ~3.5 in Cu relative to the silicate (Corgne *et al*., 2008). In our model, the core forms first, and sequesters Cu, hence $[Cu]_{core}$ should be at least 3.5x greater than that of the mantle before removal of the HM. Figure S-5 shows the relationship between $[Cu]_{core}$ and effective $D^{Cu}_{metal\text{-}Sil}$ for all the models – the curve suggests that, to be above 3.5, the core should contain at least ~120 ppm Cu, limiting the scenarios (see Fig. 3a).

Once [Cu] for core and HM are fixed, the Cu isotope evolution of the mantle can be modelled, again following two stage model. The Cu isotope mass balance between the primordial mantle (PM; that is, the mantle after core formation but before Hadean Matte segregation) and core is related to the bulk Earth composition as such:

$$\delta^{65}Cu_{CBE} = f^{Cu}_{core} \cdot \delta^{65}Cu_{core} + \left(1 - f^{Cu}_{core}\right) \cdot \delta^{65}Cu_{PM} \qquad \text{[Eq. S-4]}$$

where CBE is Chondritic Bulk Earth, as estimated in SI Section 4 ($\delta^{65}Cu_{CBE}$ = –0.19 ± 0.10 ‰). Although we do not know the absolute Cu isotope composition of the core, we can replace this term with the metal-silicate fractionation factor, $\Delta^{65}Cu_{m\text{-}s}$, estimated using the experiments (here we assume a slightly positive $\Delta^{65}Cu_{m\text{-}s}$ of +0.10 ‰, Table S-10), where:

$$\Delta^{65}Cu_{m-s} = \delta^{65}Cu_{core} - \delta^{65}Cu_{PM} \qquad \text{[Eq. S-5]}$$

Substituting Equation S-5 into S-4 and rearranging gives the simple expression:

$$\delta^{65}Cu_{PM} = \delta^{65}Cu_{CBE} - f^{Cu}_{core} \cdot \Delta^{65}Cu_{m-s} \qquad \text{[Eq. S-6]}$$

As $\Delta^{65}Cu_{m\text{-}s}$ is positive, this results in a primordial mantle that has a lighter Cu isotope composition than CBE ($\delta^{65}Cu$ = –0.26 ‰; Figure 2 in main text). If we were to instead assume that all Cu was delivered post metal-silicate equilibration by the giant impact, this is where the story starts. Assuming an enstatite chondrite-like impactor, this would set the composition of Earth's mantle to $\delta^{65}Cu_{ECBE}$ = -0.24 ± 0.09 ‰, 2 s.d. This is also slightly lighter than CBE and, in fact, identical to our predicted primordial (post-core formation) Cu isotope composition.

To reach the current mantle (BSE) Cu isotope composition, the subsequent removal of Cu into the HM should preferentially remove the lighter isotopes. The composition of the HM needed to balance BSE vs. PM can therefore be calculated:

$$\delta^{65}Cu_{PM} = \frac{\delta^{65}Cu_{PM} - \left(1 - f^{Cu}_{HM} \cdot \delta^{65}Cu_{BSE}\right)}{f^{Cu}_{HM}} \qquad \text{[Eq. S-7]}$$

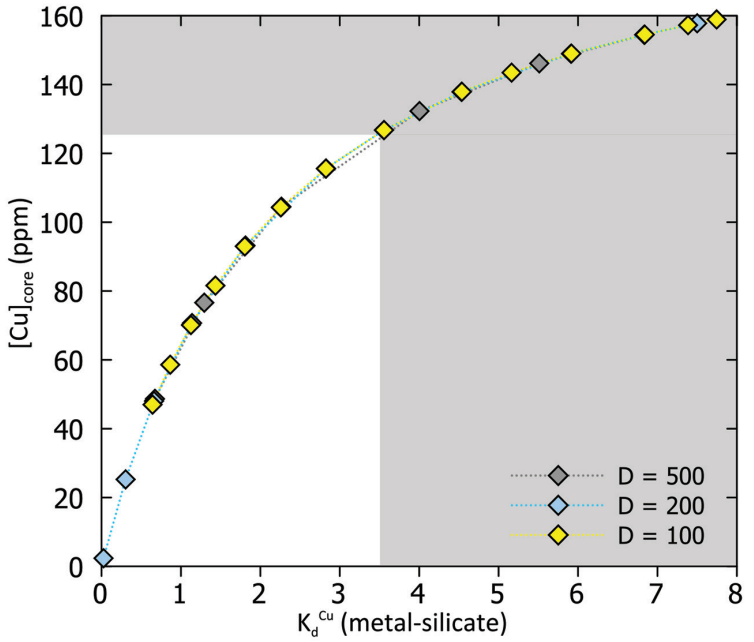

Figure S-5 Relationship between calculated Cu in core (as a result of increasing thickness of HM) and apparent D^{Cu} metal silicate values – this value should be at least greater than 3.5, which equates to >120 ppm Cu in the core. D = $D^{Cu}_{sulfide\text{-}silicate}$ therefore, for BSE [Cu] = 20 ppm, D = 500→$[Cu]_{HM}$ = 10000; D = 200→$[Cu]_{HM}$ = 4000; D = 100→$[Cu]_{HM}$ = 2000.

The range of $\delta^{65}Cu_{HM}$ values for the various allowed scenarios in Fig 3a are shown in Figure S-6. These can be converted into $\Delta^{65}Cu_{sil\text{-}s}$ values. Although we have no constraints on this value except that it will be negative relative to BSE, at mantle temperatures, $\Delta^{65}Cu_{sil\text{-}s} > 3$ ‰ may be unrealistic. Therefore, only those solutions where $\Delta^{65}Cu_{sil\text{-}s} < 2$ ‰ are shown in the main text (Fig. 3b).

7. Chemical consequences of forming the Hadean Matte on Earth's mantle and core

We choose a relatively thick layer for the HM (30 km) predicted by our models, in order to constrain the maximum elemental and isotopic effects. In terms of major element composition of the HM, we assume a stoichiometric Fe-O-S mixture, whereby the HM is composed of ~54 wt. % Fe, ~15 wt. % O and ~31 % wt. % S.

Iron is a major element in the mantle; hence, a 30 km thick HM layer, composed of 54 % Fe by mass, would only represent <1 % of Earth's Fe budget, and ~7 % of the non-metallic terrestrial Fe. The effect on mantle O abundance is smaller (<<1 % of mantle O).

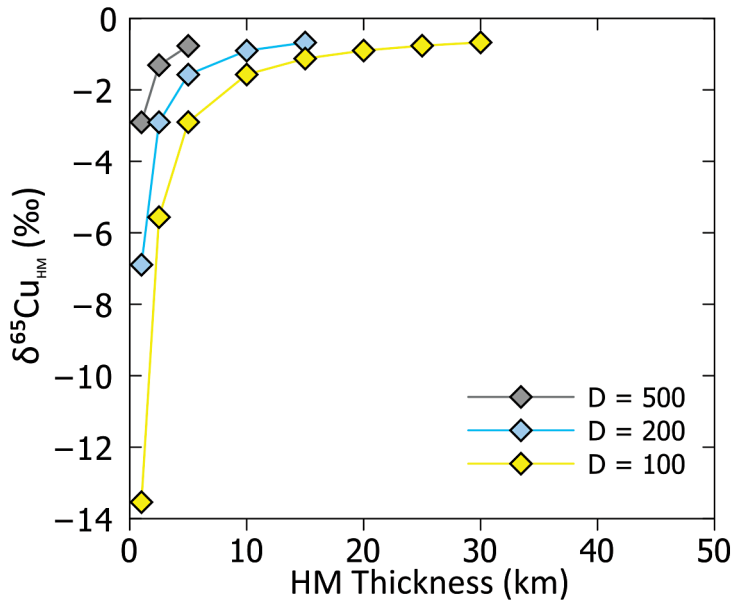

Figure S-6 Relationship between thickness of Hadean Matte and Cu isotope composition, for various $[Cu]_{HM}$ concentrations. As the thickness reduces, the isotope composition of the HM becomes more extreme, toward very light values.

In terms of assessing the impact of admixing the HM into the core, obviously, the effect on core Fe content is insignificant. With respect to O, admixing of a 30 km thick HM would add 0.25 wt. % O to the core.

The current elemental and isotopic S composition of the mantle is compatible with the formation of the HM. This is because experiments suggest that most, if not all, of primordial S was removed from the mantle during planetary differentiation, into either the metal or sulphide phase (O'Neill, 1991). The current (relatively low) S content of the mantle is thought to have been delivered during late accretion by volatile-rich impactors, based on the chondritic S isotope composition of most mantle-derived rocks (Chaussidon *et al.*, 1991). Any S remaining in the primordial mantle, post core formation, would be isotopically light relative to chondrites, as metal-silicate S fractionation preferentially enriches the metal in the heavier isotopes (Shahar *et al.*, 2009). This would mean that, if remaining primordial S was removed from the mantle by a Fe-O-S layer, it would have an isotopically light composition. Admixing the HM into the core is predicted to add up to 0.6 wt. % S to the core.

The effect on mantle Pb isotope composition

There is a long-standing conundrum regarding the Pb isotope composition of the BSE, in that, in $^{206}Pb/^{204}Pb$ vs. $^{207}Pb/^{204}Pb$ space, most mantle-derived rocks, continental sediments, etc. plot to the right of the terrestrial geochron (either the meteorite 4.568 Ga geochron or the later Hf-W core formation cessation age of ~4.53 Ga, Fig. 4 in main text). This means that most terrestrial mantle-derived samples have an overabundance of radiogenic ^{206}Pb. Assuming that Earth has an identical primordial Pb (and U) isotope budget to meteorites, there must be some complementary unradiogenic reservoir. However, there is no consensus over what this reservoir could be. This is known as the first terrestrial Pb paradox (Allègre, 1969).

Regardless of the existence of the Pb paradox, the silicate Earth has to have evolved with a higher μ (μ = $^{238}U/^{204}Pb$) than that predicted for a chondritic bulk Earth (μ ~ 1, Allègre *et al.*, 1995) to explain the overall high modern day $^{206}Pb/^{204}Pb$ and $^{207}Pb/^{204}Pb$ ratios in silicate samples. To explain the predicted modern day BSE μ values of between 8 and 10, the silicate Earth has to have roughly 60× less ^{204}Pb than bulk Earth. One way to fractionate U and Pb is via core formation – this is because Pb is both siderophile and chalcophile at conditions relevant to core formation (Bouhifd *et al.*, 2013) whereas U is lithophile.

The possibility of U/Pb fractionation as a result of core formation led to a possible solution to the Pb paradox (Allègre *et al.*, 1982, Galer and Goldstein, 1996). Specifically, a younger age for the Pb isotope system, *e.g.*, 4.468 Ga, is invoked - in this case, the Pb geochron is less steep and passes through the centre of the MORB/OIB arrays. The younger "Pb age" of the silicate Earth is often cited to represent the cessation of core formation. The main issue with this interpretation is that the Hf-W age of core formation and the Pb age of core formation do not agree – with the Pb age consistently younger (~100 Ma after the Solar System formation) than the Hf-W age (~35 Ma). To explain this, some workers have posited that the Hf-W age reflects the bulk of core segregation, whereas the Pb age reflects a late stage addition of S-rich material into the core (Wood and Halliday, 2010). This fits well with the Hadean Matte hypothesis. Here, we model the Pb isotope evolution of the mantle with 2 fractionation events (as with our mantle Cu isotope model).

Our model follows that of Galer and Goldstein (1996), and calculates ingrowth of uranogenic Pb as a result of increasing μ values as ^{204}Pb is removed first into the core at 50 Ma, then into the 30 km-thick HM at 100 Ma. We take a bulk Earth ^{204}Pb concentration of 700 ppb and that of the present day mantle of 104 ppb. Using this latter value, we can use previously determined values of $D^{Pb}_{S\text{-}sil}$ to predict the ^{204}Pb concentration in the HM, and then by mass balance calculate the amount of ^{204}Pb needed to reside in the core before HM formation. Values for $D^{Pb}_{S\text{-}sil}$ are all >1, but vary somewhat; here, we choose a value of 50, based on two more recent studies (Li and Audetat, 2012; Wood *et al.*, 2008). This gives ^{204}Pb = 5200 ppb in the HM, and ~ 1900 ppb in the core. Calculating the apparent metal-silicate D^{Pb} from these concentrations gives a value of ~13, which

is in agreement with the recent estimates (Wood *et al.*, 2008). Starting with a bulk Earth μ of ~0.9, core formation would increase mantle μ to ~6.1, then HM would further increase this to ~8.5.

Figure 4 in the main text shows the evolution of mantle Pb isotope composition for this 2-stage fractionation model. The insert shows the growth curve of mantle Pb at the intersection with the terrestrial geochron, as well as a selection of Pb isotope BSE estimates (Halliday, 2004) and flood basalt compositions, which are thought to best represent the ancient primitive mantle (Jackson and Carlson, 2011). The figure shows that our model matches fairly well some of the more unradiogenic estimates of Pb isotope mantle composition, which indicates that formation of a 30 km thick HM could explain the first Pb paradox. However, if the true Pb isotope composition of the mantle is more radiogenic (*i.e.*, the bulk of the estimates plotted in Fig. 4), this leaves the door open for further unradiogenic Pb reservoirs.

Supplementary Information References

Allègre, C.J. (1969) Comportement des systemes U-Th-Pb dans le manteau superieur et modele d'evolution de ce dernier au cours des temps geologiques. *Earth and Planetary Science Letters* 5, 261-269.

Allègre, C.J., Dupré, B., Brévart, O. (1982) Chemical aspects of the formation of the core. *Philosophical Transactions of the Royal Society of London Series A* 306, 49-59.

Allègre, C.J., Manhes, G., Göpel, C. (1995) The age of the Earth. *Geochimica et Cosmochimica Acta* 59, 1445-1456.

Archer, C., Vance, D. (2004) Mass discrimination correction in multiple-collector plasma source mass spectrometry: an example using Cu and Zn isotopes. *Journal of Analytical Atomic Spectrometry* 19, 656-665.

Barrat, J.A., Zanda, B., Moynier, F., Bollinger, C., Liorzou, C., Bayon, G. (2012) Geochemistry of CI chondrites: Major and trace elements, and Cu and Zn Isotopes. *Geochimica et Cosmochimica Acta* 83, 79-92.

Ben Othman, D., Luck, J.M., Bodinier, J.L., Arndt, N.T., Albarède, F. (2006) Cu–Zn isotopic variations in the Earth's mantle. *Geochimica et Cosmochimica Acta* 70, A46.

Bigalke, M., Kobza, J., Weyer, S., Wilcke, W. (2010) Stable Cu and Zn isotope ratios as tracers of sources and transport of Cu and Zn in contaminated soil. *Geochimica et Cosmochimica Acta* 74, 6801-6813.

Bouhifd, M.A., Andrault, D., Bolfan-Casanova, N., Hammouda, T., Devidal, J.L. (2013) Metal–silicate partitioning of Pb and U: Effects of metal composition and oxygen fugacity. *Geochimica et Cosmochimica Acta* 114, 13–28.

Chaussidon, M., Sheppard, S., Michard, A. (1991) Hydrogen, sulphur and neodymium isotope variations in the mantle beneath the EPR at 12°50′N. In: Taylor, H.P., O'Neil, J.R., Kaplan, I.R. (Eds.) *Stable Isotope Geochemistry: a Tribute to Samuel Epstein*. *Geochemical Society Special Publication* 3, 325–337.

Corgne, A., Keshav, S., Wood, B.J., McDonough, W.F., Fei Y. (2008) Metal–silicate partitioning and constraints on core composition and oxygen fugacity during Earth accretion. *Geochimica et Cosmochimica Acta* 72, 574-589.

Fellows, S.A., Canil, D. (2012) Experimental study of the partitioning of Cu during partial melting of Earth's mantle. *Earth and Planetary Science Letters* 337-338, 133-143.

Fitoussi, C., Bourdon, B. (2012) Silicon isotope evidence against an enstatite chondrite earth. *Science* 335, 1477-1480.

Gaetani, G.A., Grove, T.L. (1997) Partitioning of moderately siderophile elements among olivine, silicate melt, and sulphide melt: Constraints on core formation in the Earth and Mars. *Geochimica et Cosmochimica Acta* 61, 1829-1846.

Galer, S.J.G., Goldstein S.L. (1996) Influence of accretion on lead in the Earth. In: Basu, A., Hart, S. (Eds.) *Earth Processes: Reading the Isotopic Code*, *AGU Geophysical Monograph* 95, 75-98.

Halliday, A.N. (2004) Mixing, volatile loss and compositional change during impact-driven accretion of the Earth. *Nature* 427, 505-509.

Herwartz, D., Pack, A., Friedrichs, B., Bischoff, A. (2014) Identification of the giant impactor Theia in lunar rocks. *Science* 344, 1146-1150.

Ikehata, K., Hirata, T. (2012) Copper Isotope Characteristics of Copper-Rich Minerals from the Horoman Peridotite Complex, Hokkaido, Northern Japan. *Economic Geology* 107, 1489-1497.

Jackson, M.G., Carlson, R. (2011) An ancient recipe for flood basalt genesis. *Nature* 476, 316-319.

Keil, K. (1989) Enstatite meteorites and their parent bodies. *Meteoritics and Planetary Science* 24, 195-208.

Kiseeva, E.S., Wood, B.J. (2013) A simple model for chalcophile element partitioning between sulphide and silicate liquids with geochemical applications. *Earth and Planetary Science Letters* 383, 68-81.

Larner, F., Rehkämper, M., Coles, B.J., Kreissig, K., Weiss, D.J., Sampson, B., Unsworth, C., Strekopytov, S. (2011) A new separation procedure for Cu prior to stable isotope analysis by MC-ICP-MS. *Journal of Analytical Atomic Spectrometry* 26, 1627–1632.

Lee, C.-T.A., Yin, Q.-Z., Lenardic. A., Agranier, A., O'Neill, C.J., Thiagarajan, N. (2007) Trace-element composition of Fe-rich residual liquids formed by fractional crystallization: Implications for the Hadean magma ocean. *Geochimica et Cosmochimica Acta* 71, 3601-3615.

Lee, C.-T.A., Luffi, P., Chin, E.J., Bouchet, R., Dasgupta, R., Morton, D.M., Le Roux, V., Yin, Q.-Z., Jin, D. (2012) Copper systematics in arc magmas and implications for crust-mantle differentiation. *Science* 335, 64-66.

Li, W., Jackson, S.E., Pearson, N.J., Alard, O., Chappell, B.W. (2009) Cu isotopic signature of granites from the Lachlan Fold Belt, SE Australia. *Chemical Geology* 258, 38-49.

Li, Y., Audétat, A. (2012) Partitioning of V, Mn, Co, Ni, Cu, Zn, As, Mo, Ag, Sn, Sb, W, Au, Pb, and Bi between sulphide phases and hydrous basanite melt at upper mantle conditions. *Earth and Planetary Science Letters* 355-356, 327–340.

Liu, S.-A., Li, D., Li, S., Teng, F.-Z., Ke, S., He, Y., Lu, Y. (2014) High-precision copper and iron isotope analysis of igneous rock standards by MC-ICP-MS. *Journal of Analytical Atomic Spectrometry* 29, 122-133.

Lodders, K. (2000) An oxygen isotope mixing model for the accretion and composition of rocky planets. *Space Science Reviews* 92, 341-354.

Luck, J.-M., Ben Othman, D., Barrat, J.A., Albarède, F. (2003) Coupled ^{63}Cu and ^{16}O excesses in chondrites. *Geochimica et Cosmochimica Acta* 67, 143-151.

Luck, J.M., Ben Othman, D., Albarède, F. (2005) Zn and Cu isotopic variations in chondrites and iron meteorites: Early solar nebula reservoirs and parent-body processes. *Geochimica et Cosmochimica Acta* 69, 5351-5363.

Maréchal, C.N., Télouk, P., Albarède, F. (1999) Precise analysis of copper and zinc isotopic compositions by plasma-source mass spectrometry. *Chemical Geology* 156, 251-273.

Markl, G., Lahaye, Y., Schwinn, G. (2006) Copper isotopes as monitors of redox processes in hydrothermal mineralization. *Geochimica et Cosmochimica Acta* 70, 4215-4228.

McDonough, W.F. (2003) Compositional model for the Earth's core. In: Carlson, R.W. (Ed.) *The mantle and core*, *Treatise on Geochemistry*, 1st edition, 2, 547-568.

Moeller, K., Schoenberg, R., Pedersen, R.-B., Weiss, D., Dong, S. (2012) Calibration of the New Certified Reference Materials ERM-AE633 and ERM-AE647 for Copper and IRMM-3702 for Zinc Isotope Amount Ratio Determinations. *Geostandards and Geoanalytical Research* 36, 177-199.

Moynier, F., Koeberl, C., Beck, P., Jourdan, F., Telouk, P. (2010) Isotopic fractionation of Cu in tektites. *Geochimica et Cosmochimica Acta* 74, 799-807.

O'Neill, H.St.C. (1991) The origin of the moon and the early history of the earth - A chemical model. Part 2: The earth. *Geochimica et Cosmochimica Acta* 55, 1159-1172.

Palme, H., O'Neill, H.St.C. (2014) Cosmochemical estimates of mantle composition. In: Carlson, R.W. (Ed.) *The mantle and core, Treatise on Geochemistry*, 2nd edition, 3, 1-39.

Poitrasson, F., Roskosz, M., Corgne, A. (2013) No iron isotope fractionation between molten alloys and silicate melt to 2000 °C and 7.7 GPa: Experimental evidence and implications for planetary differentiation and accretion. *Earth and Planetary Science Letters* 278, 376-385.

Puchtel, I.S., Hofmann, A.W., Mezger, K., Shchipansky, A.A., Kulikov, V.S., Kulikova, V.V. (1996) Petrology of a 2.41 Ga remarkably fresh komatiitic basalt lava lake in Lion Hills, central Vetreny Belt, Baltic Shield. *Contributions to Mineralogy and Petrology* 124, 273-290.

Puchtel, I.S., Walker, R.J., Brandon, A.D., Nisbet, E.G. (2009) Pt–Re–Os and Sm–Nd isotope and HSE and REE systematics of the 2.7 Ga Belingwe and Abitibi komatiites. *Geochimica et Cosmochimica Acta* 73, 6367-6389.

Shahar, A., Fei, Y., Liu, M.C., Wang, J. (2009) Sulfur isotopic fractionation during the differentiation of Mars. *Geochimica et Cosmochimica Acta* 73, A1201.

Siebert, J., Corgne, A., Ryerson, F.J. (2011) Systematics of metal-silicate partitioning for many siderophile elements applied to Earth's core formation. *Geochimica et Cosmochimica Acta* 75, 1451-1489.

Stracke, A., Hofmann, A.W., Hart, S.R. (2005) FOZO, HIMU and the rest of the mantle zoo. *Geochemistry, Geophysics, Geosystems* 6.

Thibault, Y., Walter, M.J. (1995) The influence of pressure and temperature on the metal-silicate partition coefficients of nickel and cobalt in a model C1 chondrite and implications for metal segregation in a deep magma ocean. *Geochimica et Cosmochimica Acta* 59, 991-1002.

Williams, H.M., Archer, C. (2011) Copper stable isotopes as tracers of metal-sulphide segregation and fractional crystallisation processes on iron meteorite parent bodies. *Geochimica et Cosmochimica Acta* 75, 3166-3178.

Wood, B.J., Halliday, A.N. (2010) The lead isotopic age of the Earth can be explained by core formation alone. *Nature* 465, 767-770.

Wood, B.J., Nielsen, S.G., Rehkämper, M., Halliday, A.N. (2008) The effects of core formation on the Pb- and Tl- isotopic composition of the silicate Earth. *Earth and Planetary Science Letters* 269, 326–336.